Christie, D.M., Pedersen, R.B., Miller, D.J., et al., 2001
Proceedings of the Ocean Drilling Program, Initial Reports Volume 187

15. SITE 1164[1]

Shipboard Scientific Party[2]

PRINCIPAL RESULTS

Site 1164 is located 100 km northeast of Site 1163 on seafloor of magnetic age 18–19 Ma. The site is located in a small sediment-filled ridge-parallel basin, midway between the ~126°E and the ~127°E fracture zones that bound Segment B5. This is the southernmost of three sites selected to test the distribution of Pacific- and Indian-type mantle beneath Segment B5. It also lies on a time line (±1 m.y.) with Site 1163 (Segment B4) and Site 1162 (Zone A). The purpose of this final Segment B5 site was to further constrain the emerging pattern of short-lived migrations of the Indian/Pacific mantle boundary.

Hole 1164A was spudded in 4798 m water depth. We washed through ~138.5 m of sediment, recovering 0.7 m of drilling-disturbed, densely packed, light brown to very light brown carbonate-rich clay containing small (millimeter sized) chips of basalt, basaltic glass, and palagonite. Rotary drilling continued the hole 8.5 m into volcanic basement, recovering 0.97 m (11.4%) of aphyric pillow basalt. The basalt is slightly to moderately altered, with Fe oxyhydroxide, clay, and carbonate replacing phenocryst phases and groundmass. Hole 1164A was abandoned because of poor drilling conditions.

Hole 1164B was spudded 200 m to the southwest of Hole 1164A and was washed through ~150.4 m of sediment, recovering 0.8 m of carbonate-rich clay and two basalt pieces. Rotary drilling continued 65.7 m into basement, recovering 10.65 m (16.2%) of aphyric basalt rubble with intervals of basaltic breccia. The basalts are moderately to highly altered with Fe oxyhydroxide and clay as the typical alteration products.

Two glass samples were analyzed for major and trace elements using the onboard inductively coupled plasma–atomic emission spectrometry (ICP-AES); two whole-rock powders were analyzed by X-ray fluorescence (XRF). As at all other Leg 187 sites, the whole rocks contain less

[1]Examples of how to reference the whole or part of this volume.
[2]Shipboard Scientific Party addresses.

Ms 187IR-115

MgO than the glasses, most likely as a result of Mg loss during alteration. The Ba and Zr contents of one glass lie within the Indian field defined by 0- to 7-Ma mid-ocean-ridge basalts (MORBs) from the Southeast Indian Ridge (SEIR), whereas the other glass sample plots within the Pacific field. Both plot close to the field boundaries and close to the tie line connecting axial samples from present-day Segment B5. This suggests that the mantle beneath Site 1164 is transitional in character, similar to that beneath Segment B5 at present.

OPERATIONS

Transit to Site 1164

We made the 51-nmi northeast transit between Sites 1163 and 1164 at average speed of 11.3 kt. At 1130 hr on 3 January, we slowed to 6 kt and ran a southwest-to-northeast single-channel seismic (SCS) survey over the prospectus site to confirm sediment thickness. We dropped a positioning beacon on the prospectus Global Positioning System (GPS) coordinates.

Hole 1164A

The corrected precision depth recorder (PDR) depth referenced to the dual-elevator stool at this site is 4809.4 m. The nine-collar bottom-hole assembly employed at the previous sites was reassembled with a new C-4 four-cone rotary bit made up to a refurbished mechanical bit release. We initiated Hole 1164A at 2145 hr on 3 January. After washing through 138.5 m of sediment and recovering a wash barrel (Core 187-1164A-1W; Table T1), we cored to 146.7 meters below seafloor (mbsf) before drilling conditions forced us to abandon the hole. We recovered four cores (Cores 187-1164A-2R to 4R), although the last core was probably material recovered during our attempt to ream the hole and clear several meters of fill. A bag with fluorescent microsphere tracers was deployed in the core catcher of Core 187-1164A-2R. The bit cleared the seafloor at 1115 hr, and we offset 200 m back along our survey track to the southwest.

T1. Coring summary, Site 1164, p. 45.

Hole 1164B

Hole 1164B was spudded with the rotary core barrel at 1230 hr on 4 January. We washed down to 150.4 mbsf at 50 m/hr and retrieved the core barrel (Core 187-1164B-1W) when the driller noted a hard contact. We advanced the hole by rotary coring to 216.1 mbsf, recovering nine cores (Cores 187-1164B-2R to 10R). Microsphere tracers were deployed on Cores 187-1164B-2R and 10R. Hole conditions and recovery were not ideal, but we continued operations until we reached our nominal depth objective. The drill string cleared the seafloor at 0045 hr and the rotary table at 0845 on 6 January, ending operations for Leg 187.

IGNEOUS PETROLOGY

Introduction

Holes 1164A and 1164B were rotary cored into igneous basement from 138.5 to 147.0 mbsf and 150.4 to 215.9 mbsf, respectively. Hole

1164A (Sections 187-1164B-2R-1 through 4R-1) was drilled 8.5 m into basement, resulting in 0.97 m of recovered core (equal to 11.41% recovery). All recovered material from the basement core has been assigned to one lithologic unit: aphyric basalt. Based on the high proportion of glassy chilled margins recovered (i.e., 33% of the pieces), the rocks are interpreted to be pillow lavas.

Hole 1164B (Sections 187-1164B-1W-1 through 10R-1) was drilled 65.7 m into basement, resulting in 10.65 m of recovered core (equal to 16.21% recovery). This hole yielded basaltic rubble, consisting predominantly of highly altered aphyric basalt, with two intervals of basaltic breccia. The material was assigned to a single unit: basaltic rubble. Based on the abundance of chilled margins recovered, the presence of V-shaped pieces, radial fractures, and chilled margins with arcuate shapes, the material is interpreted as being derived from a pillow basalt flow.

Hole 1164A

Unit 1

All of the basement rocks recovered in Hole 1164A have been assigned to a single lithologic unit consisting of a slightly altered, light gray, aphyric basalt (Fig. F1). The rocks contain rare (<0.5%) phenocrysts of plagioclase (as long as 3 mm) and euhedral phenocrysts/microphenocrysts of olivine (as large as 1.5 mm); the latter is commonly replaced by Fe oxyhydroxides and clay in alteration halos and by calcite (Fig. F2) in less altered interiors of pieces (see "Hole 1164A," p. 7, in "Alteration"). Prismatic plagioclase is seriate, with crystals ranging from ~2 mm long to microlites ~0.1 mm, although most crystals are <~1 mm in length.

Groundmass phases fall into two textural categories. Approximately 50% of the rock is made up of microcrystalline plumose quench crystals (Fig. F3) that are predominantly intergrowths of clinopyroxene and plagioclase ± olivine. The rest consists of microphenocrysts and/or prismatic groundmass plagioclase intimately intergrown with anhedral clinopyroxene in a subophitic texture (Fig. F4). These clusters are not xenocrysts but equilibrium intergrowths, as clinopyroxene is also observed as a euhedral microphenocryst phase (Fig. F3) and is the only mafic groundmass phase identified in the available thin section for this unit (Sample 187-1164A-4R-1, 20–22 cm). This indicates that these basalts are multiply saturated with olivine, plagioclase, and clinopyroxene. Clinopyroxene ranges from anhedral crystals (as large as 0.6 mm) in the crystal clusters to equant groundmass crystals (<25 µm); plagioclase ranges from prismatic to tabular crystals ~1 mm long to acicular and skeletal microlites ~30 µm long (Figs. F3, F4). The prismatic crystals typically have narrow embayments in the cores that are elongated parallel to cleavage (Fig. F4), which is consistent with growth from skeletal crystals during cooling. Proportions of groundmass phases are difficult to estimate because of the predominance of microcrystalline quench morphologies, but plagioclase and clinopyroxene are probably present in roughly equal amounts. Aside from microphenocrysts, olivine was not positively identified in the groundmass. Dark brown interstitial material (altered glass + cryptocrystalline quench phases) makes up ~10% of the rock. Minute (<20 µm) equant opaque minerals form <2% of the groundmass.

F1. Aphyric basalt typical of Unit 1, p. 13.

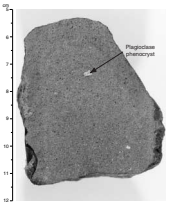

F2. Olivine phenocryst partially replaced by calcite, p. 14.

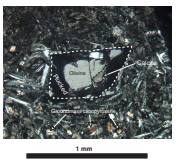

F3. Euhedral clinopyroxene microphenocryst, p. 15.

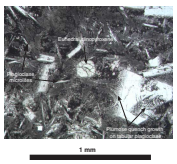

F4. Subophitic clinopyroxene + plagioclase clusters, p. 16.

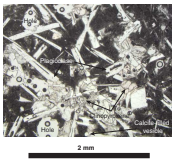

Small vesicles as large as 2 mm in diameter represent ~1% of the rock. In hand specimen, most of these appear to be either unfilled or lined with blue cryptocrystalline silica/clay, calcite, Fe oxyhydroxides, Mn oxide, or light green clays. In thin section, however, many are observed to have been infilled with quench crystals that are finer grained than the surrounding groundmass (Fig. F5). Some of these "refilled" vesicles also have secondary calcite in the center (Fig. F5; see "Hole 1164A," p. 7, in "Alteration").

Chilled margins were recovered on three pieces (33%) from this unit. In all cases the thickness of clear glass is small (<2 mm), and most of what is retained is spherulitic quench crystals + glass, partially altered to palagonite. The zone of coalesced spherulites is relatively thin (2–3 mm), and the spherulites are small (~100–200 µm in diameter).

F5. Vesicles filled by melt drainback, p. 17.

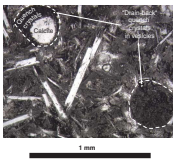

Hole 1164B

Unit 1

Unit 1 of Hole 1164B consists of basaltic rubble with two intervals of basaltic breccia: Section 187-1164B-R-1 (Pieces 7–12) and Section 187-1164B-4R-2 (Pieces 13–15). Three igneous lithologies are present in the rubble: (1) moderately plagioclase-olivine phyric basalt, (2) sparsely plagioclase-olivine phyric basalt, and (3) aphyric basalt with plagioclase and olivine microphenocrysts. The moderately plagioclase-olivine phyric basalts are present only at the top of the basement section (Sections 187-1164B-1W-2 through 3R–1) and represent 2% of the core. These are among the least-altered rocks recovered in Hole 1164B, being slightly to moderately altered (see "Hole 1164B," p. 8, in "Alteration"). The sparsely plagioclase-olivine phyric basalts, which make up 8% of the core, are most common from Sections 187-1164B-3R-1 through 4R-1; below this, only aphyric basalts were recovered (i.e., 87% of the core). Furthermore, the sparsely plagioclase-olivine phyric basalts and the aphyric basalts appear to be part of a lithologic continuum that straddles the boundary between our applied definition of aphyric and phyric (see "Igneous Petrology," p. 4, in "Explanatory Notes" and "Aphyric [to Sparsely Plagioclase-Olivine Phyric] Basalts," p. 5). Therefore, these two lithologies will be discussed together and, for brevity, will be referred to simply as aphyric basalt.

In contrast to the moderately plagioclase-olivine phyric basalts, ~55% of the aphyric basalts are highly altered and 25% are moderately altered (see "Hole 1164B," p. 8, in "Alteration"). This high degree of alteration, along with the small size of most pieces and the recovery of basaltic breccia in Sections 187-1164B-3R-1 and 4R-2, is the basis for the interpretation of the unit as a rubble pile. However, the aphyric basalts in Section 187-1164B-10R-1, which are lithologically indistinguishable from the aphyric basalts elsewhere in Hole 1164B, are significantly less altered than the overlying rocks and there are fewer small (i.e., <~4–5 cm) round pieces. This suggests that the rubble intervals may be part of a relatively intact sequence of pillow lavas.

F6. Moderately plagioclase-olivine phyric basalt, p. 18.

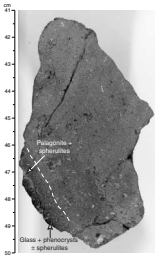

Petrography of Basaltic Rubble

Moderately Plagioclase-Olivine Phyric Basalts. These basalts (Fig. F6) consist of 1%–2% equant olivine and 1%–4% prismatic to tabular plagioclase phenocrysts. Plagioclase ranges from 1 to 5 mm and olivine from 1 to 4 mm. Approximately 10% of the phenocrysts are included in glomerocrysts. These range from loose clusters of prismatic plagioclase

(2–3 crystals; <~1 mm long) + small equant to skeletal olivine (1–3 crystals; <~0.2 mm) to more tightly intergrown glomerocrysts of prismatic to tabular plagioclase crystals (10–20 crystals; ~0.5–1 mm long). Larger plagioclase phenocrysts (3–4 mm) display discontinuous zoning and are sieve textured, some extensively (Fig. F7). These textures clearly indicate partial resorption and disequilibrium with the host basalt. Smaller prismatic crystals have narrow embayments parallel to cleavage or twin planes and are unzoned, consistent with development of these features during crystal growth. All plagioclase phenocrysts show albite twinning and are generally unaltered. Equant olivine phenocrysts range from subhedral to euhedral; they are altered to Fe oxyhydroxides in alteration halos but elsewhere are either unaltered or partially replaced by a yellow to white clay. Cr spinel is present in trace amounts as small (~30µm) euhedral inclusions in olivine and as discrete subhedral crystals as large as 0.4 mm.

Groundmass textures are microcrystalline, ranging from intersertal to sheaf quench crystal morphologies. Acicular to skeletal plagioclase forms ~40% of the groundmass and equant olivines (<~0.5 mm) form 2%–3% of the groundmass. Clinopyroxene is present predominantly as plumose quench crystals intergrown with plagioclase, but anhedral, granular crystals as large as ~50 µm are present adjacent to and within miarolitic cavities; these cavities are commonly filled with secondary clay or calcite (see **"Hole 1164B,"** p. 8, in "Alteration"). Fe-Ti oxides are present as minute (<10 µm) equant crystals and constitute ~1%–2% of the groundmass. Dark brown mesostasis—which here includes glass + indistinguishable quench crystals of plagioclase, clinopyroxene, and olivine—constitutes >50% of the rock. Vesicles vary in size and abundance, ranging from as large as 1 mm in diameter, forming ~1% of the rock, to rare (<<1%) and small (<~0.5 mm). They are spherical and tend to be lined or filled with blue to white cryptocrystalline silica/clay or Fe oxyhydroxides (see **"Hole 1164B,"** p. 8, in "Alteration").

Aphyric (to Sparsely Plagioclase-Olivine Phyric) Basalts. These basalts (Fig. F8) contain ≤1% prismatic to tabular plagioclase phenocrysts and 1%–5% olivine microphenocrysts. In most samples, prismatic plagioclase is seriate, with crystals ranging from ~2 mm long to microlites ~0.1 mm. This makes distinguishing groundmass crystals from phenocrysts somewhat arbitrary, and categorizing the rock as aphyric or as sparsely plagioclase-olivine phyric basalt is often a question of whether a sufficient number of crystals exceeds ~1 mm in size. The problem of visually estimating the modal proportions of phases in hand specimen is exacerbated by (1) the high degree of alteration of most pieces, which tends to overemphasize the abundance of both olivine and plagioclase crystals (Figs. F9, F10) and (2) the tendency for the crystals to occur as glomerocrysts, which can lead to overestimations of size (Figs. F11, F12). In general, the abundance of plagioclase and olivine crystals larger than 1 mm is <1%. We therefore consider the rocks to be aphyric, containing rare phenocrysts of plagioclase + microphenocrysts of olivine.

Although most plagioclase crystals tend to be small and prismatic (<1 mm long), anhedral tabular crystals as large as 3 mm are observed in a few pieces (e.g., Sample 187-1164B-5R-1 [Piece 5]). Approximately 10%–20% of the phenocrysts and microphenocrysts are included in glomerocrysts or clusters (Figs. F11, F12). All plagioclase phenocrysts show albite twinning and are generally unaltered. Equant olivine microphenocrysts (<1 mm) are relatively abundant (3%–5%) and range from subhedral to euhedral. Fresh olivine is rarely observed; however, it is totally

F7. Sieve-textured plagioclase, p. 19.

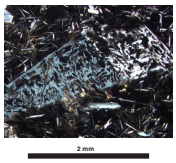

F8. Aphyric basalt clast typical of this lithology, p. 20.

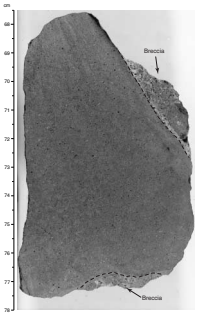

F9. Aphyric basalt clast in basaltic breccia, p. 21.

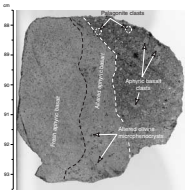

F10. Highly altered sparsely plagioclase-olivine phyric basalt, p. 22.

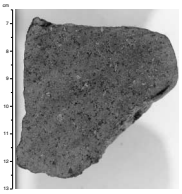

F11. Plagioclase + olivine glomercryst (loose cluster), p. 23.

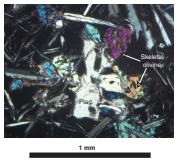

replaced by Fe oxyhydroxides and clay in most moderately to highly altered samples (see **"Hole 1164B,"** p. 8, in "Alteration").

Groundmass textures are microcrystalline, ranging from intersertal to sheaf quench crystal morphologies. Skeletal acicular to prismatic plagioclase forms ~30%–40% of the groundmass. Dark brown quench-textured mesostasis makes up ~50% of most rocks (Fig. **F11**), but a few samples show a slightly greater degree of clinopyroxene growth (Fig. **F13**). Although the groundmass is still microcrystalline, the clinopyroxene is present in bundles of bladed crystals (~10 µm wide) that are generally in optical continuity. Enhanced clinopyroxene crystal growth also occurs within miarolitic cavities, where clinopyroxene forms subhedral to euhedral crystals as long as 250 µm (Fig. **F13**). Similarly, Fe-Ti oxides make up ~1% of the groundmass and are generally present as minute (<2 µm) equant crystals concentrated in areas of mesostasis. However, within miarolitic cavities they may reach sizes of 50 µm.

Vesicles are small (<300 µm in diameter) and rare; most are unfilled or lined with a white to blue cryptocrystalline clay/silica. In the less highly altered areas of some pieces, they are filled with calcite or clay (see **"Hole 1164B,"** p. 8, in "Alteration"). In contrast, miarolitic cavities are common (3%–5% of the rock). They are generally filled with clear sparry calcite or clay, but in Sample 187-1164B-5R-1, 100–104 cm, they are filled with an inclusion-filled calcite that has a bladed habit and shows sweeping extinction (Fig. **F14**).

Chilled Margins. Chilled margins were recovered on 45 rubble clasts (i.e., 18% of the pieces); two are phyric basalts (e.g., Fig. **F6**) and the rest are aphyric. In spite of the overall high degree of alteration of the unit, fresh glass was preserved on a large number of pieces. Rinds of clear glass typically range from 1 to 10 mm in thickness; this is followed by 1–2 mm of glass and discrete spherulites. Inward from the glassy rind, the chilled margin typically consists of a 5-mm-wide zone of coalesced spherulites; the glass interstitial to the spherulites in this zone is replaced by palagonite in most samples. Based on the overall abundance of chilled margins among the rubble pieces, the presence of pieces with classic V shapes and radial fractures (e.g., Fig. **F15**), and the presence of arcuate chilled margins (e.g., Sample 187-1164B-8R-1 [Piece 19]), the basalts in Hole 1164B are inferred to have originated as a sequence of pillow basalts.

Petrography of the Breccia

There are two breccia intervals in Hole 1164B (i.e., Section 187-1164B-3R-1 [Pieces 7–12], Fig. **F16;** Section 4R-2 [Pieces 13–15]; Fig. **F17**). The sediments in these two intervals are similar in that both are poorly sorted and dominated by lithic clasts of aphyric basalt and palagonite ± glass. Angular clasts of slightly to moderately altered basalt dominate the >5-mm range. Some of these clasts have concentric alteration halos, but most do not, indicating that little postdepositional alteration has occurred (see **"Alteration,"** p. 7). Since sediment is found adhering to several long basalt pieces (Figs. **F16, F18**), the maximum clast size for the deposit is significantly greater than the diameter of the core.

In spite of the similarities described above, the proportions of the different lithic clasts differ within the two breccias. In Section 187-1164B-3R-1, for example, subrounded clasts of yellow palagonite ± glass and white clay after palagonite dominate the 1–3-mm range. Indeed, clasts of palagonite may form as much as ~60% of the rock, since the matrix is a honey brown clay to silt, probably derived from the breakdown of

F12. Plagioclase glomerocryst, p. 24.

F13. Bladed habit of groundmass clinopyroxene adjacent to a miarolitic cavity, p. 25.

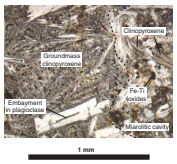

F14. Miarolitic cavity with a multistage filling history, p. 26.

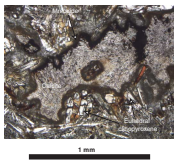

F15. Arcuate chilled margin on an aphyric pillow basalt clast, p. 27.

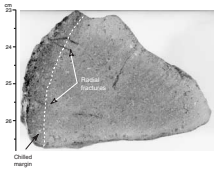

F16. Palagonite-rich basaltic breccia adhering to aphyric basalt, p. 28.

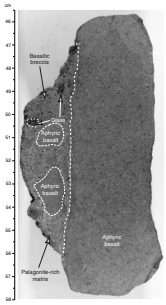

palagonite clasts. In addition, the sediment in this interval is loosely cemented by clay and/or quartz, and some pieces in Section 187-1164B-3R-1 have drusy to botryoidal quartz lining pore spaces. There is no indication of sorting by density or size.

In contrast, yellow palagonite and white clay form <25% of the 1–3-mm range for the breccias in Section 187-1164B-4R-2. Although most have concentric rims of yellow palagonite or white clay, clasts of unaltered glass are common, as is unaltered olivine (Fig. F19). The matrix is composed predominantly of gray to white, silt- to sand-sized particles of uncertain origin (Fig. F20), but it probably originates from the breakdown of basalt, glass, and plagioclase rather than from palagonite. Thus, the breccia from this interval has a dark black appearance throughout. Sample 187-1164B-4R-2, 65–69 cm, also shows inverse size grading (Fig. F18). This piece has a subvertical, tube-shaped pocket (2.5 cm × 1 cm × 0.5 cm) in which a buff-colored clay and silt layer (1–5 mm thick) lines the pocket, grading into a 2.5-cm pocket of sand-sized lithic clasts, composed mostly of palagonite and glass.

Both breccias differ significantly from the basalt-carbonate breccias recovered previously at Sites 1157, 1160, and 1162, since carbonate is absent from the sediment in Hole 1164B. The abundance of unaltered olivine and glass and the absence of carbonate cements or large amounts of clay suggest that these breccias formed in a sediment-starved setting. They probably do not represent a significant amount of sedimentary transport and may instead have formed by autobrecciation of pillows during eruption. In contrast to the high degree of alteration of the surrounding rubble clasts, the relatively unaltered state of these sediments suggests that fluid flow through them has been negligible.

ALTERATION

Hole 1164A

Aphyric basalt from Hole 1164A has been slightly to moderately altered at low temperature. In some places, small patches of clay or Fe oxyhydroxide and spots (<0.5 mm) or dendritic patches of Mn oxide cover the outer surfaces of pieces. The fracture plus vein density is comparatively low, 4.5/m. The few fractures present are <0.3 mm wide, free of alteration halos, and either lined or filled with whitish blue cryptocrystalline silica ± Mn oxide. The highest degree (15%–30%) of alteration occurs in 1- to 20-mm-wide halos that are aligned subparallel to piece or chilled margins (e.g., Section 187-1164-2R-1 [Piece 1]). Broader alteration halos are subdivided into outer and inner zones. The outer zones are as wide as 15 mm and altered to grayish brown; they are characterized by pervasive replacement of groundmass and total replacement of olivine microphenocrysts by Fe oxyhydroxide and clay. The inner zones are narrower (3–5 mm) and less altered to dark gray; these are characterized by patchy groundmass replacement and partial (20%–50%) replacement of olivine microphenocrysts by Fe oxyhydroxide and clay. Lining or filling of vesicles with cryptocrystalline silica, calcite, Fe oxyhydroxide, green clays, and Mn oxide occurs mainly in the alteration halos. A sharp boundary separates the alteration halos from the light gray fresher interiors. Calcite (<1%) replaces groundmass, fills miarolitic cavities, (Fig. F21) and replaces olivine microphenocrysts in the fresher interiors of pieces (Fig. F22). Quenched pillow margins are present

F17. Palagonite-poor basaltic breccia clast, p. 29.

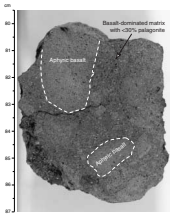

F18. Aphyric basalt with adhering clastic sediments, p. 30.

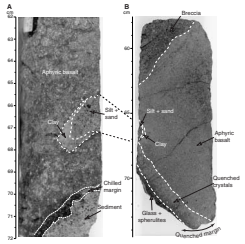

F19. Palagonite-poor basaltic breccia, p. 31.

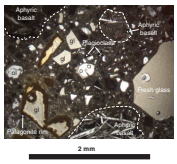

F20. Photomicrograph of basaltic breccia matrix, p. 32.

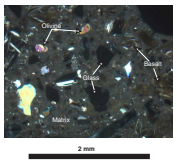

F21. Patchy calcite replacing groundmass or filling a vug, p. 33.

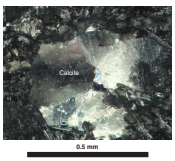

F22. Olivine phenocryst partially replaced by calcite, p. 34.

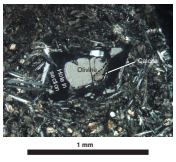

throughout the core. These typically consist of 1- to 3-mm-wide zones of fresh glass covered by 0.5 mm layers of orange-brown palagonite.

Hole 1164B

Subrounded basalt pieces with outer surfaces weathered to yellowish brown are present throughout the core. Together with an unsystematic intermixture of aphyric and slightly phyric basalts (Sections 187-1164-1W-2 through 4R-1), this suggests that a rubble deposit was sampled (see "Igneous Petrology," p. 2). The sparsely plagioclase-olivine phyric basalt, aphyric basalt, and basalt breccia from Hole 1164B were subject to pervasive low-temperature alteration. About 85% of the rock from this hole is highly (~55%) or moderately (~30%) altered (Table T2). The least-altered rocks (i.e., where >50% of each piece is classified as slightly altered) are restricted to Sections 187-1164B-1W-1, 1W-2, and 10R-1. Six veins were recorded, giving a fracture plus vein density of 10/m of core. Fractures are rare; where present, they are usually lined with Mn oxide and, in places, with Fe oxyhydroxide or clay. Very minor small veins (<0.2 mm) are mostly filled with Mn oxide. Veins and fractures do not have substantial alteration halos. Vesicles are rare throughout (<1%); where present, they are 0.3–0.5 mm and spherical, and most are unfilled.

T2. Relative abundance of altered basalt pieces, p. 46.

Highly Altered Basalts

The highly (40%–80%) altered basalts are characterized by an intense brown coloration. These are either pervasively altered (Fig. F23) or have alteration halos that extend 10–30 mm into piece interiors and make up >60% of individual pieces. Within these halos, alteration is progressively less intense toward the interior of individual pieces. The alteration halos are characterized by 30%–60% replacement of the groundmass by Fe oxyhydroxide and clay. Pieces with more pervasive groundmass alteration (>50% of the groundmass is replaced by Fe oxyhydroxide and clay) have more intense brown coloration. Groundmass olivine (Fig. F23), clinopyroxene, and mesostasis (Fig. F24) are commonly altered, whereas plagioclase is fresh throughout except for Mn oxide staining. In addition, 2- to 4-mm-sized irregularly shaped patches of Mn oxide replace groundmass phases (Fig. F25). Olivine phenocrysts are totally replaced by Fe oxyhydroxide and clay; plagioclase phenocrysts are occasionally stained black by Mn oxide or yellowish by Fe oxide but are otherwise fresh. Within the alteration halos or in pieces with pervasive groundmass replacement, some vesicles are lined with cryptocrystalline silica and/or Fe oxyhydroxide or filled with clay.

F23. Sparsely plagioclase-olivine phyric basalt, p. 35.

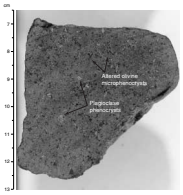

F24. Pervasively altered groundmass of an aphyric basalt, p. 36.

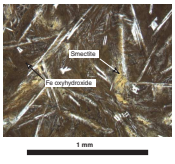

Moderately Altered Basalts

Moderately altered basalts have grayish brown interiors rimmed by comparatively thin alteration halos (1.5–5 cm) making up <60% of each piece. Within the alteration halos, the groundmass is mostly replaced (30%–60%) by Fe oxyhydroxide and clay, as it is in the highly altered pieces. The most clearly visible expressions of groundmass alteration are olivine microphenocrysts, altered completely to reddish brown Fe oxyhydroxide and clay. Within the fresher interiors of pieces, patchy areas of groundmass (1–8 mm across) are replaced by Fe oxyhydroxide and clay. Olivine phenocrysts are 100% replaced by Fe oxyhydroxide and clay, whereas plagioclase phenocrysts are mostly fresh. Some vesi-

F25. Pillow basalt with patchy replacement of groundmass by Mn oxide, p. 37.

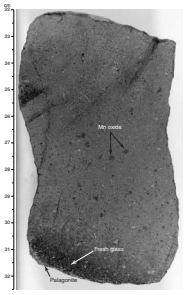

cles within the alteration halos are lined with cryptocrystalline silica and/or Fe oxyhydroxide or filled with clay.

Slightly Altered Rocks

The few slightly altered rocks (Table T2) typically have alteration halos 1 to 10 mm wide aligned subparallel to the piece margins; these halos do not exceed 30% of the total volume of individual pieces. Within alteration halos, the groundmass is 20%–50% replaced by Fe oxyhydroxide and clay. In many cases, the alteration of olivine microphenocrysts to Fe oxyhydroxide and clay within the alteration halos makes it difficult to distinguish phyric from aphyric basalt. This is because fresh, transparent olivine microphenocrysts are not readily visible relative to the dark groundmass of slightly altered pieces (Fig. F9).

In the fresher, light to medium gray interior of some pieces, miarolitic cavities are commonly lined by Mn oxide and filled with calcite (Fig. F14). Calcite is the most abundant secondary mineral in the interiors of slightly altered pieces. In contrast, calcite is almost entirely absent from the moderately and highly altered pieces. This suggests that calcite deposition takes place at the initial stages of low-temperature alteration. Chilled margins are present in most sections. Fresh glass rinds range from <1 to 10 mm in thickness (Fig. F25), usually with associated orange-brown layers or small veins of palagonite.

Basalt Breccia

Glass shards make up 10%–60% in the 2- to 3-mm range of the basalt breccia in Sections 187-1164B-3R-1 and 4R-2 (see "Igneous Petrology," p. 2). Both fresh and palagonitized shards are common, suggesting that palagonitization occurred before breccia formation (Fig. F26). Palagonitized glass is commonly rimmed by dark brown palagonite that, in contrast to earlier sites, does not display dendritic textures along the palagonite/glass interface (Fig. F27).

MICROBIOLOGY

Three rock samples (187-1164B-3R-1 [Piece 11, 79–82 cm], 8R-1 [Piece 7, 28–31 cm], and 10R-1 [Piece 1, 0–4 cm]) were collected from Hole 1164B to characterize the microbial community inhabiting this environment (Table T3). All samples were pillow basalt fragments, composed of partially altered glass rinds and more crystalline interiors (see "Igneous Petrology," p. 2). Section 187-1164B-3R-1 (Piece 11) had sediment attached to a chilled margin. To sterilize them, the outer surfaces of the rocks were quickly flamed with an acetylene torch, and enrichment cultures and samples for DNA analysis and electron microscope studies were prepared (see "Igneous Rocks," p. 7, in "Microbiology" in the "Explanatory Notes" chapter).

Fluorescent microsphere tests were carried out on one basement core from Hole 1164A and two from Hole 1164B to evaluate the extent of contamination caused by drilling fluid (see "Tracer Test," p. 9, in "Microbiology" in the "Explanatory Notes" chapter and Table T3). Pieces of rock from each core were rinsed in nanopure water, and the collected water was filtered. No thin section was made from Core 187-1164A-2R because only one piece of rock was recovered. Thin sections from Hole 1164B cores were used to examine the extent of contamination inside

F26. Fresh basalt shards without palagonite rims, p. 38.

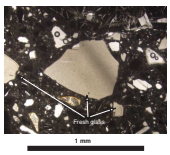

F27. Basalt glass shard with a fresh core rimmed by dark brown palagonite in basalt breccia, p. 39.

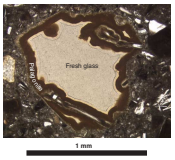

T3. Rock samples for cultures, DNA analysis, SEM/TEM, and contamination studies, p. 47.

the samples. Filters and thin sections were examined under a fluorescence microscope for the presence of microspheres. Microspheres were detected on all three filters. In the thin sections, microspheres were located both inside fractures and on thin-section surfaces. The microspheres on the polished surfaces may have been relocated by polishing. Thirty-six microspheres were observed in the thin section from Core 187-1164B-2R and 14 from Core 187-1164B-10R.

SITE GEOPHYSICS

Site selection for Site 1164 was based on a SCS survey conducted during the *R/V Melville* cruise Sojourner 5 in 1997. A 31-min SCS and 3.5-kHz PDR survey was conducted on the approach to Site 1164 (*JOIDES Resolution* [JR] SCS line S12; Fig. **F28**) to ensure the correct site location by comparing the GPS navigated SCS data with the previous SCS image and to verify sediment thickness. The ship's average speed was 6.3 kt. The water gun was triggered at a shot interval of 12 s, equivalent to ~39 m at 6.3 kt. Site 1164, with a water depth of 4809.4 m, is at the GPS coordinates of prospectus site AAD-33a (AAD = Australian Antarctic Discordance) at a position corresponding to shotpoint 136 of seismic profile S12. Note that the navigation data file is offset from seismic records by 17 shots because of a fault during the survey. The shot numbers were counted sequentially, but the navigation data were reset (i.e., shotpoint 136 on record shows as shotpoint 119 in the data). Sediment cover was estimated from 6.48 to 6.63 s in two-way traveltime, equivalent to 150 m (Fig. **F29**). We washed through 138.5 m of sediment in Hole 1164A before basement was reached, whereas in Hole 1164B, ~200 m southwest of Hole 1164A, we drilled through 150.4 m of sediment.

F28. Track chart of the SCS survey line S12, p. 40.

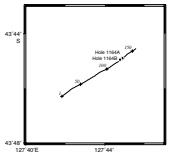

F29. SCS profile of line S12 from shotpoints 1 to 150, p. 41.

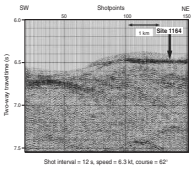

SEDIMENTS

One wash barrel was recovered from each of Holes 1164A and 1164B. Core 187-1164A-1W contains 75 cm of drilling-induced pellets and fragments of densely packed, light brown to very light brown carbonate-rich clay. From 0 to 7 cm, very fine clay pellets occur in a soupy clay matrix. From 7 to 43 cm is a very poorly sorted but normally graded interval with <1-mm to 3-cm clay fragments. Also present is a rounded piece of basalt (3 cm × 5 cm) embedded in the sediment. From 47 to 75 cm is another normally graded, poorly sorted interval of 0.5- to 3-cm drilling-induced clay fragments. Millimeter-sized chips of basalt, fresh basaltic glass, and palagonite, with and without attached indurated clay, are present throughout the section. These chips are sparse in the upper half of the section but more abundant in the lower half, where they account for 1%–2% of the core.

The wash barrel from Hole 1164B also contained carbonate-rich clay and basalt. From 0 to 29 cm in Section 187-1164B-1W-1 is soupy, very light brown carbonate-rich clay. This interval includes two 3-cm angular fragments of light brown, densely packed, stiff, carbonate-rich clay. From 29 to 39 cm in the same section is severely drilling-disturbed light brown carbonate-rich clay. The contact between these units is obscured by drilling disturbance. From 39 cm in Section 187-1164B-1W-1 to the bottom of the core-catcher section, several pieces of aphyric basalt are included in the sediment (see **"Igneous Petrology,"** p. 2).

GEOCHEMISTRY

Introduction

Site 1164 basalts were recovered from two holes that sampled 18- to 19-Ma-old crust from Segment B5 of the AAD. Two whole-rock samples were analyzed for major and trace elements by XRF only, and two samples of fresh glass chips were analyzed for major and trace elements by ICP-AES only. The results are shown in Table T4.

T4. Compositions of basalts from Site 1164, p. 48.

Hole 1164A

The samples from Hole 1164A are from a single unit of aphyric pillow basalt (see "Igneous Petrology," p. 2). Both whole rock and glass are relatively evolved, consistent with the presence of euhedral clinopyroxene phenocrysts (see "Igneous Petrology," p. 2). However, the glass has ~1.75 wt% more Fe_2O_3, ~1 wt% more MgO, ~0.1 wt% less K_2O, ~25 ppm less Sr, ~100 ppm less Ni, and ~100 ppm less Cr than the whole rock. Lower Ni and Cr contents in the glass could reflect analytical bias between the XRF and ICP-AES analyses, although ~100-ppm differences have not been observed in other whole-rock XRF-ICP sample pairs. There are smaller differences in other elements between the glass and the whole rock that appear to be mostly caused by lower MgO content in the whole rock. Nonetheless, it is difficult to attribute the differences in whole-rock and glass compositions to removal of Mg by alteration when loss-on-ignition values are <1%. Taken at face value, the glass and whole rock are not genetically related by simple low-pressure crystal fractionation.

Hole 1164B

Samples from Hole 1164B are from a single unit of pillow basalt rubble (see "Igneous Petrology," p. 2). Although aphyric basalt predominates in this hole, moderately plagioclase-olivine phyric basalt occurs at the top of the hole. Our samples are from this part of the sequence. The glass has ~0.30 wt% more TiO_2, ~1.5 wt% more Fe_2O_3, ~1 wt% more MgO, ~10 ppm more Zr, and ~0.10 wt% less K_2O than the whole rock. Smaller differences in composition between the glass and whole rock also exist for other elements. Again, the glass and whole rock compositional trends are not indicative of simple low-pressure crystal fractionation. Either Mg loss is responsible for this lack of a genetic relationship or the whole rocks are derived from parental melts that differ from the associated glass.

F30. Major element variations vs. MgO for basalts from Holes 1164A and 1164B, p. 42.

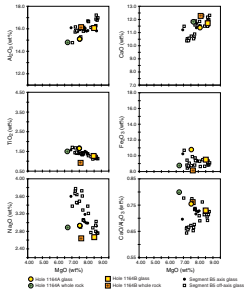

Temporal Variations

Site 1164 samples are compared to 0- to 7-Ma lavas from Segment B5 of the AAD in Figures F30 and F31. The glass samples plot within the range of younger Segment B5 basalts. The whole-rock samples are displaced from the glass trends in the TiO_2, Na_2O, Ni, and Cr vs. MgO plots. The glasses from Holes 1164A and 1164B are identical to younger Segment B5 glass; therefore, no significant difference in melting or mantle composition is inferred.

F31. Trace element variations vs. MgO for basalts from Holes 1164A and 1164B, p. 43.

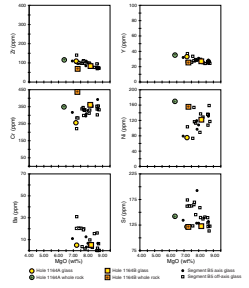

Mantle Domain

On the Zr/Ba vs. Ba diagram, Hole 1164A glass lies within the Pacific-type field and Hole 1164B glass lies within the Indian-type field. Note that both glass samples plot on the low-Ba side of the gray tie line connecting Segment B5 axial glasses that define the transition between Indian and Pacific types along the present SEIR (Fig. F32A). On the Na_2O/TiO_2 vs. MgO diagram, Site 1164 glasses also parallel samples from the B5 spreading axis but are displaced toward the Pacific-type region on the diagram (Fig. F32B). These observations suggest that Site 1164 basalts are derived from a transitional mantle, similar to that present beneath the Segment B5 axis today.

F32. Variations of Zr/Ba vs. Ba and Na_2O/TiO_2 vs. MgO for Site 1164 basalt, p. 44.

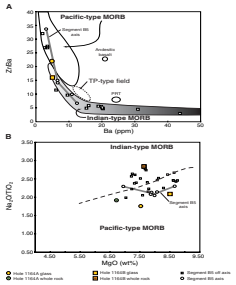

Figure F1. Photograph of interval 187-1164A-4R-1, 5–12 cm, showing an aphyric basalt with rare tabular plagioclase phenocrysts, typical of Unit 1 of Hole 1164A.

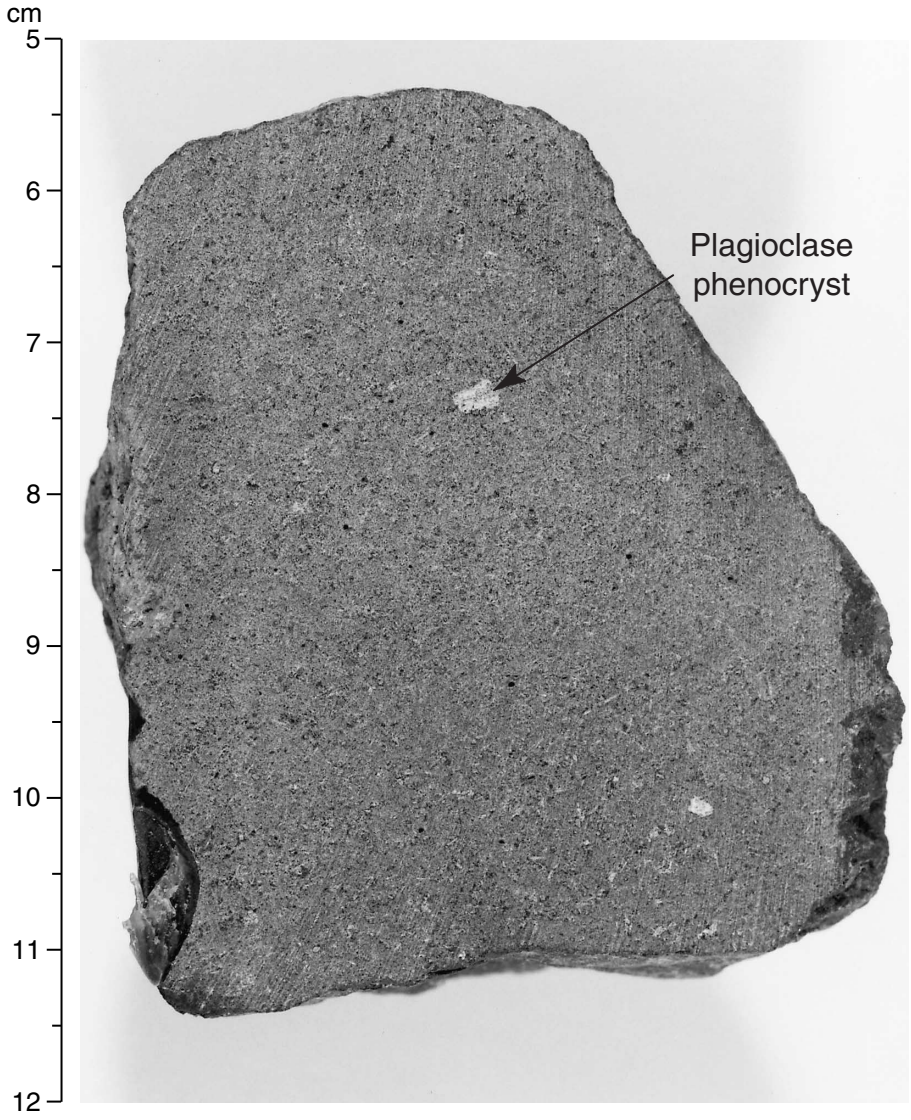

Figure F2. Photomicrograph, with crossed polars, of Sample 187-1164A-4R-1, 20–22 cm (see **"Site 1164 Thin Sections,"** p. 21), showing olivine phenocryst partially replaced by calcite. The groundmass is predominantly plumose quench-textured clinopyroxene; small birefringent crystals in the groundmass are also clinopyroxene. The dark area around the olivine is a hole produced during thin section preparation and is inferred to have been filled with calcite.

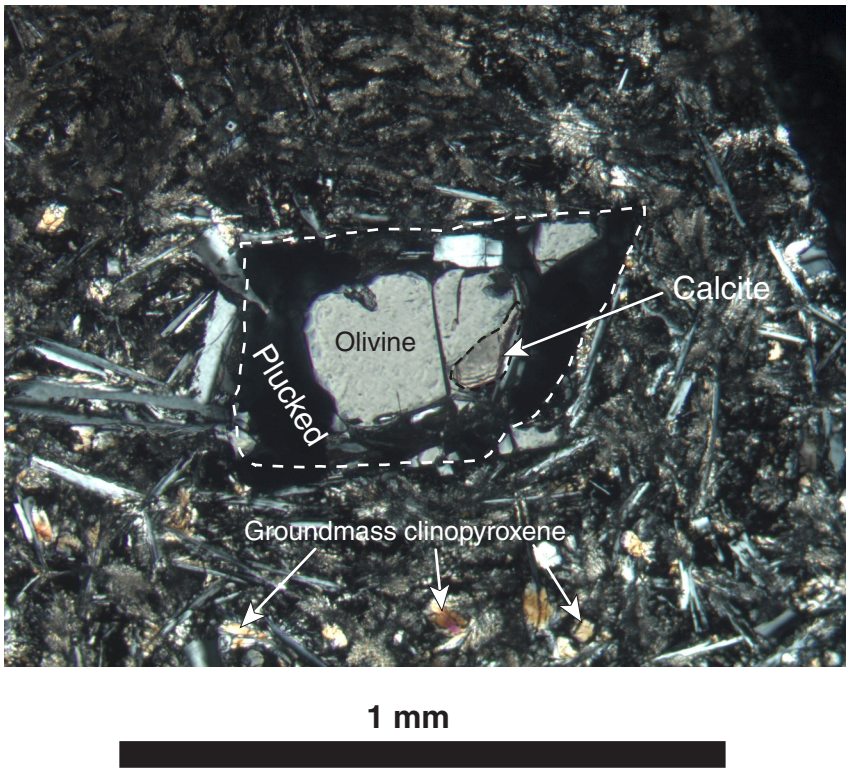

Figure F3. Photomicrograph in plane-polarized light of Sample 187-1164A-4R-1, 20–22 cm (see **"Site 1164 Thin Sections,"** p. 21), showing euhedral clinopyroxene microphenocryst in plumose groundmass quench texture typical of Unit 1 of Hole 1164A. Note the quench growth that apparently nucleated on the edges of the tabular plagioclase crystal (lower right).

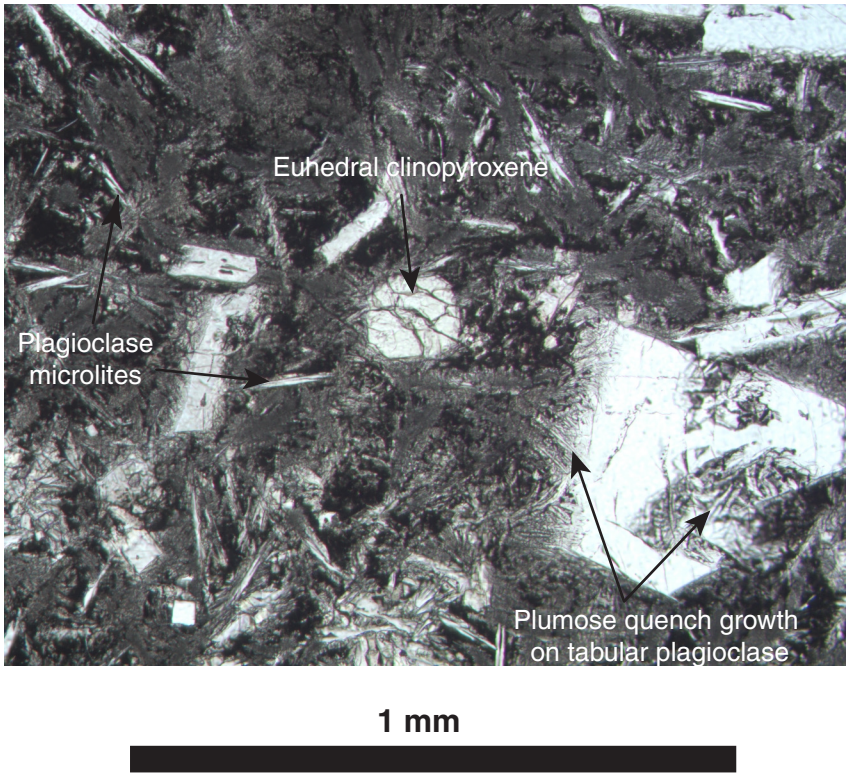

Figure F4. Photomicrograph in plane-polarized light of Sample 187-1164A-4R-1, 20–22 cm (see **"Site 1164 Thin Sections,"** p. 21), showing clinopyroxene + plagioclase clusters with subophitic textural relationship between the two phases. Note the abundance of prismatic crystals with narrow embayments parallel to twin or cleavage planes.

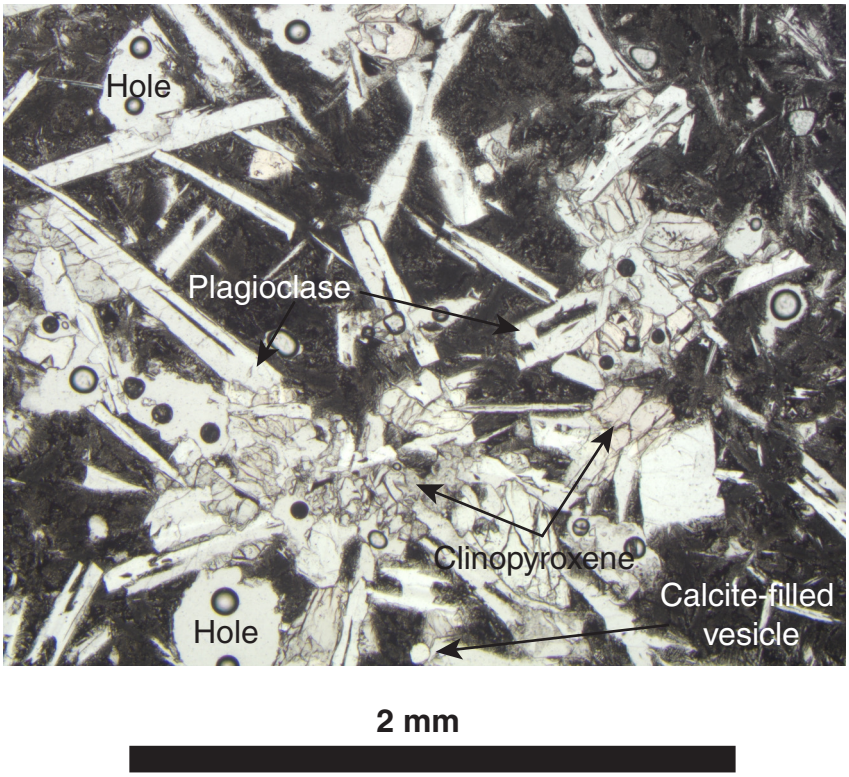

Figure F5. Photomicrograph in plane-polarized light of Sample 187-1164A-4R-1, 20–22 cm (see **"Site 1164 Thin Sections,"** p. 21), showing vesicles filled by melt drain-back, producing quenched glass and crystals that are finer grained than the surrounding groundmass. Note that the vesicle (upper left) has calcite filling the center.

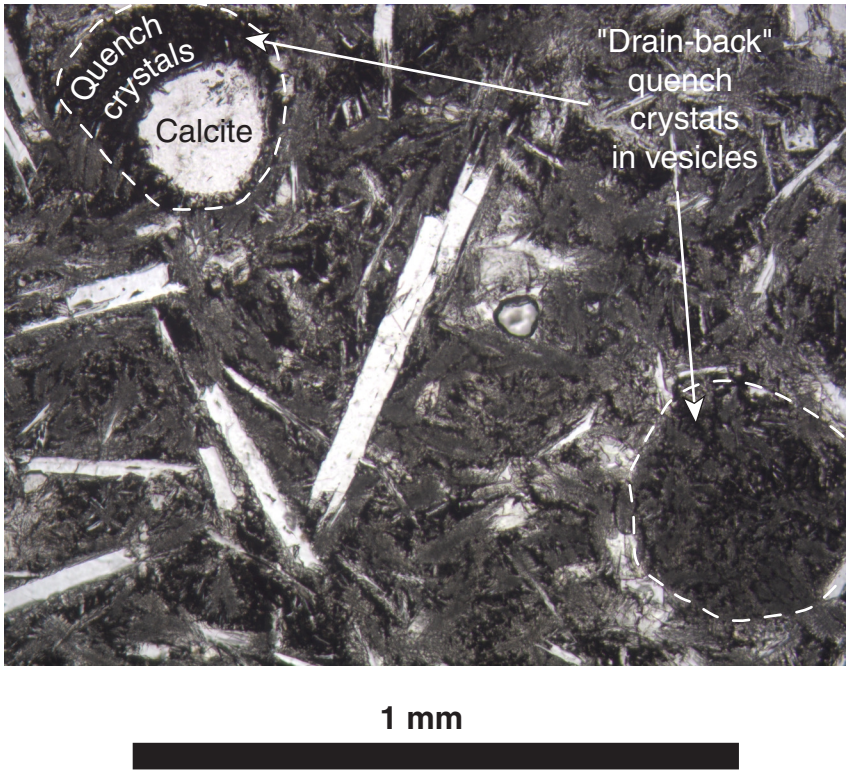

Figure F6. Photograph of interval 187-1164B-2R-1, 41–50 cm, showing moderately plagioclase-olivine phyric basalt typical of this lithology among the rubble clasts of Unit 1 of Hole 1164B. The sample has a chilled glassy margin (indicated by dashed line) on the lower left.

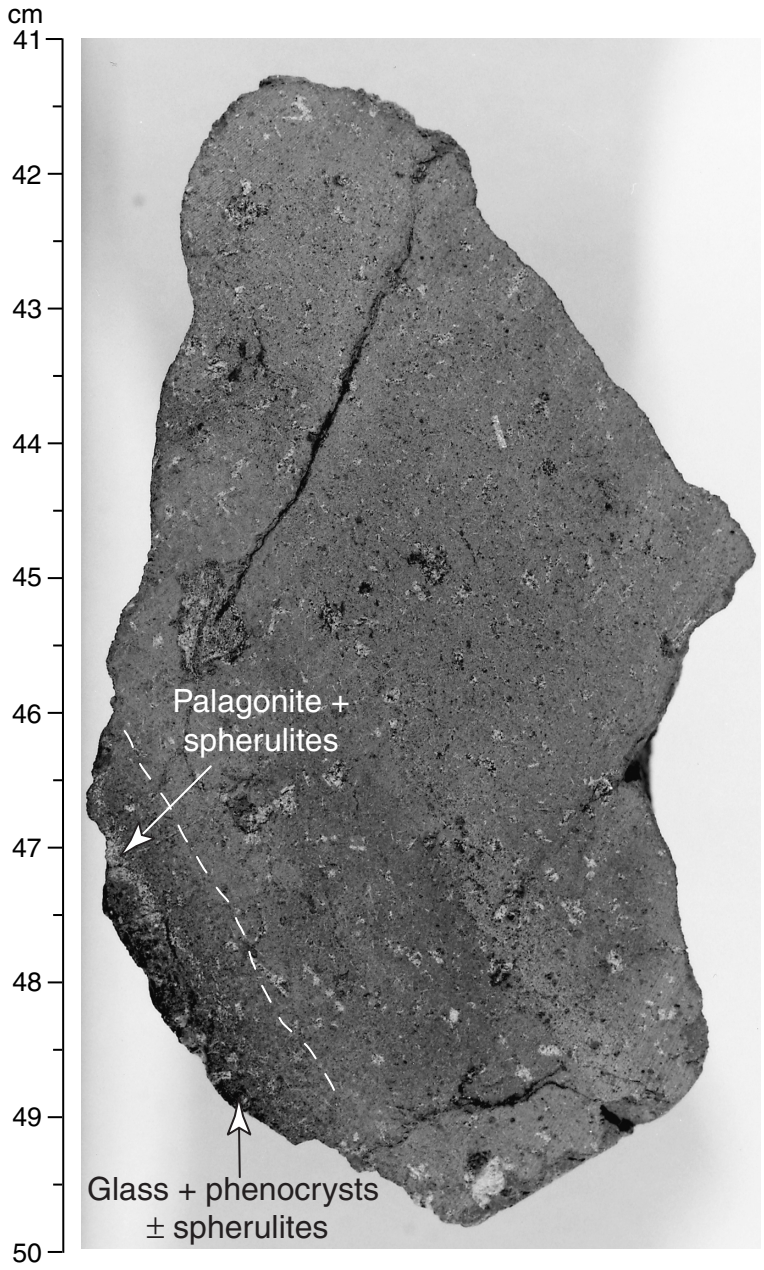

Figure F7. Photomicrograph, with crossed polars, of Sample 187-1164B-2R-1, 50–53 cm (see **"Site 1164 Thin Sections,"** p. 22) , showing sieve-textured plagioclase, indicative of partial resorption and disequilibrium with the host basalt.

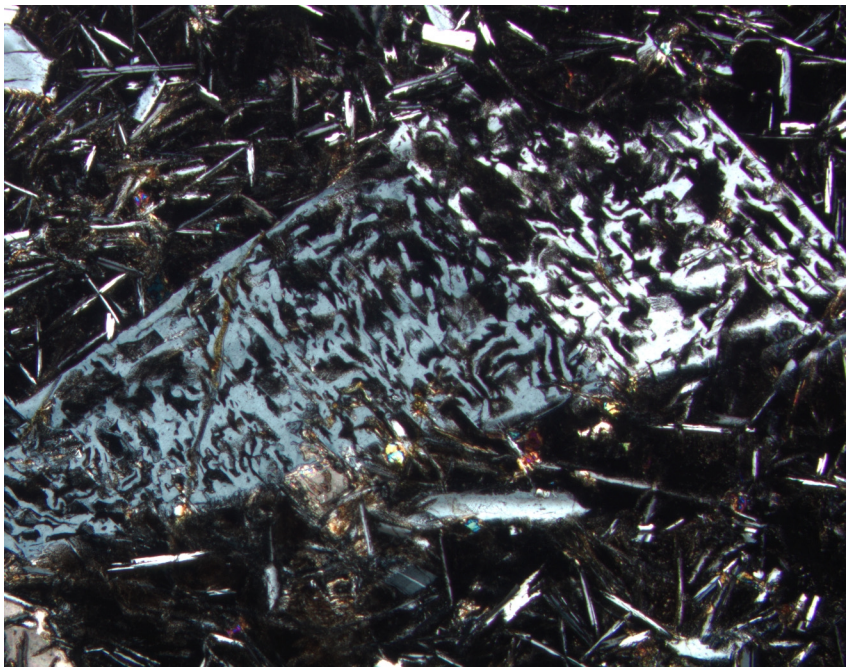

Figure F8. Photograph of interval 187-1164B-3R-1, 68–78 cm, showing a typical aphyric basalt rubble clast of Unit 1 of Hole 1164B. Note the breccia adhering to the piece (bottom and right side).

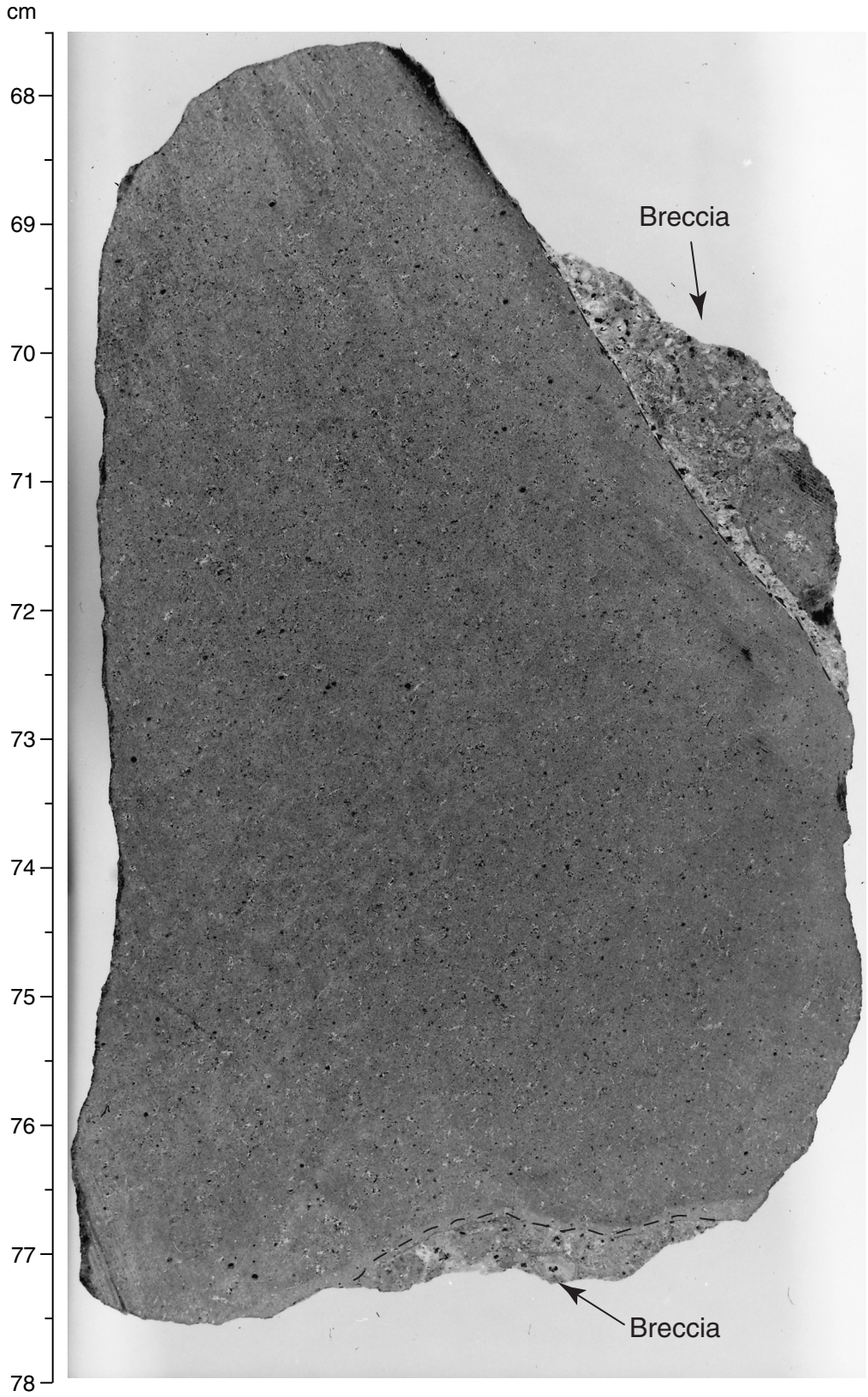

Figure F9. Photograph of interval 187-1164B-4R-2, 88–93 cm, showing a large aphyric basalt clast in basaltic breccia exhibiting the contrast in appearance of altered and unaltered areas. Olivine and plagioclase crystals are emphasized in the alteration halo adjacent to the breccia. Note the presence of numerous smaller clasts of similar aphyric basalt in the breccia.

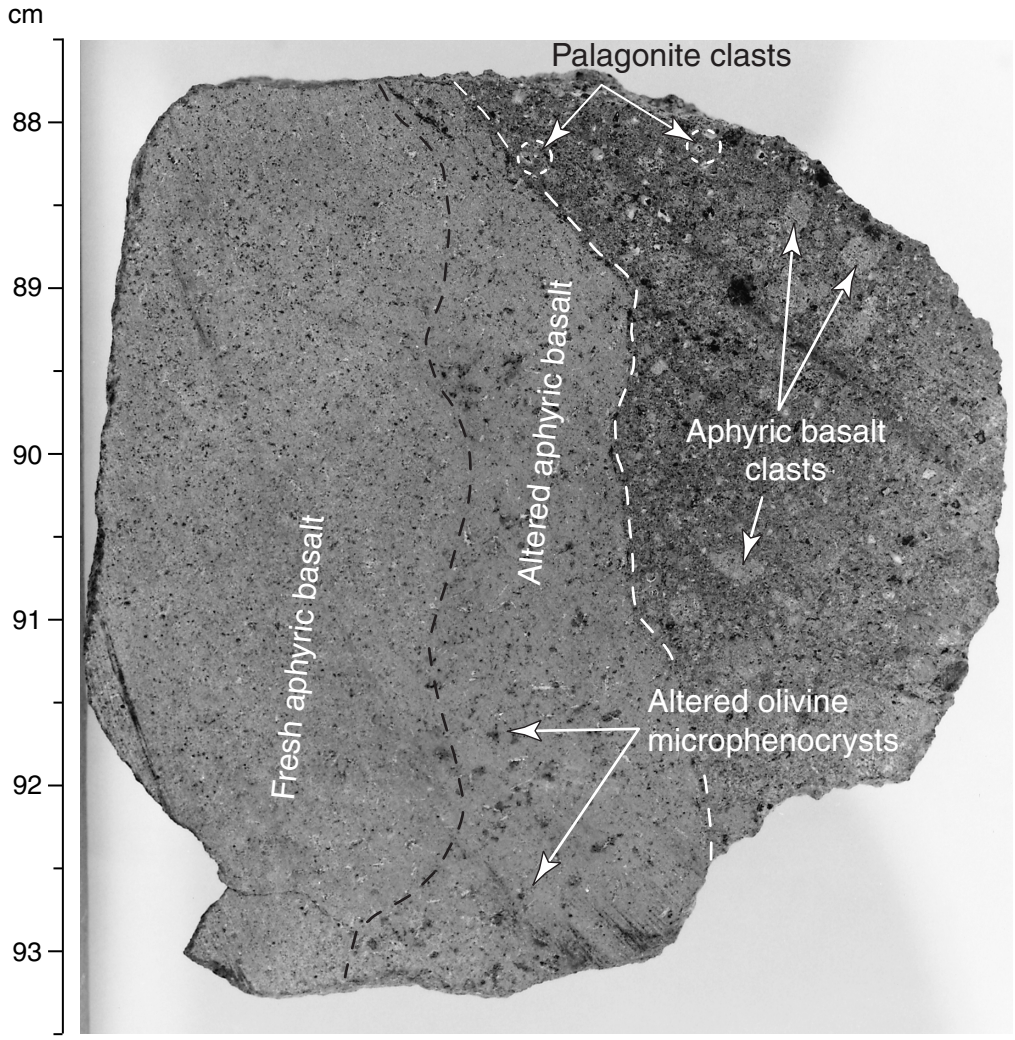

Figure F10. Photograph of interval 187-1164B-3R-2, 7–13 cm, showing highly altered sparsely plagioclase-olivine phyric basalt. Alteration emphasizes the abundance of olivine and plagioclase.

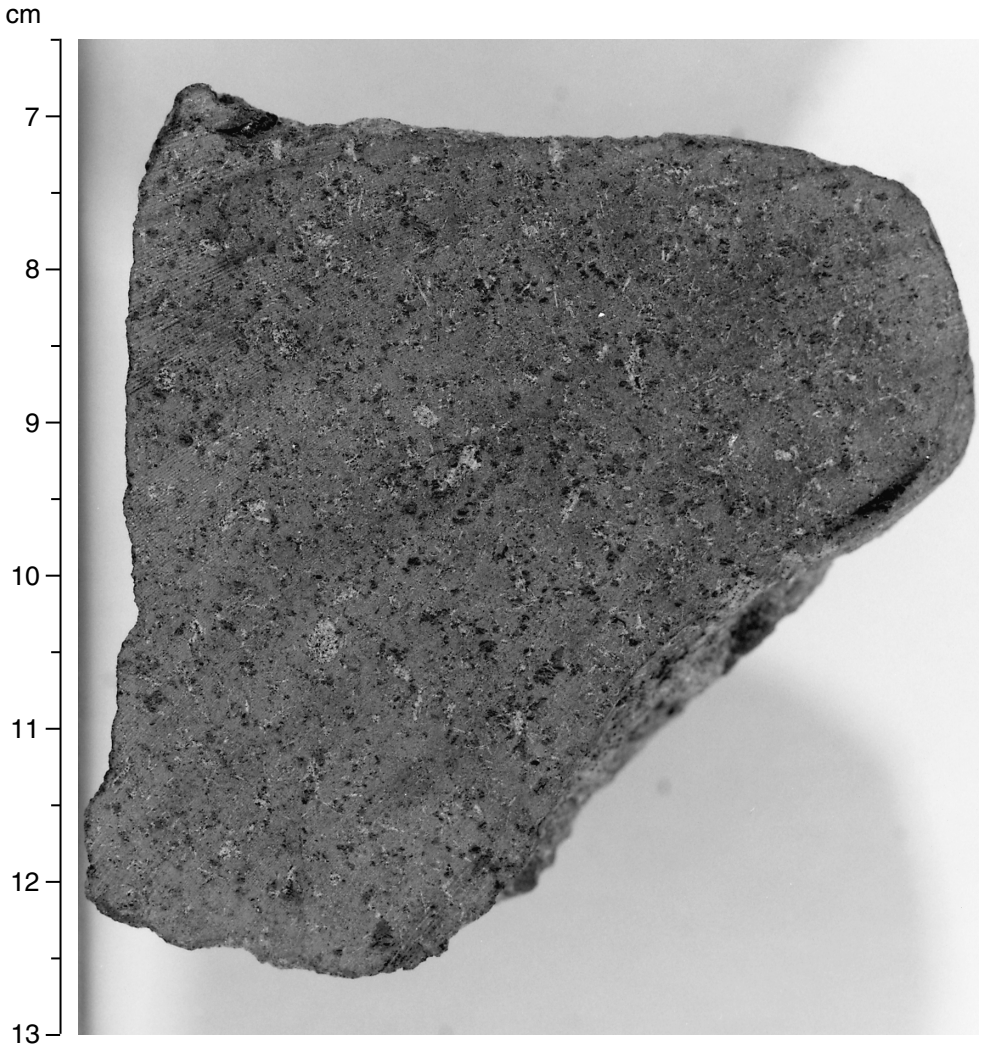

Figure F11. Photomicrograph, with crossed polars, of Sample 187-1164B-10R-1, 43–46 cm (see **"Site 1164 Thin Sections,"** p. 26), showing loose clusters of plagioclase (Plag.) and skeletal olivine formed by equilibrium crystal growth in dark brown quench-textured groundmass.

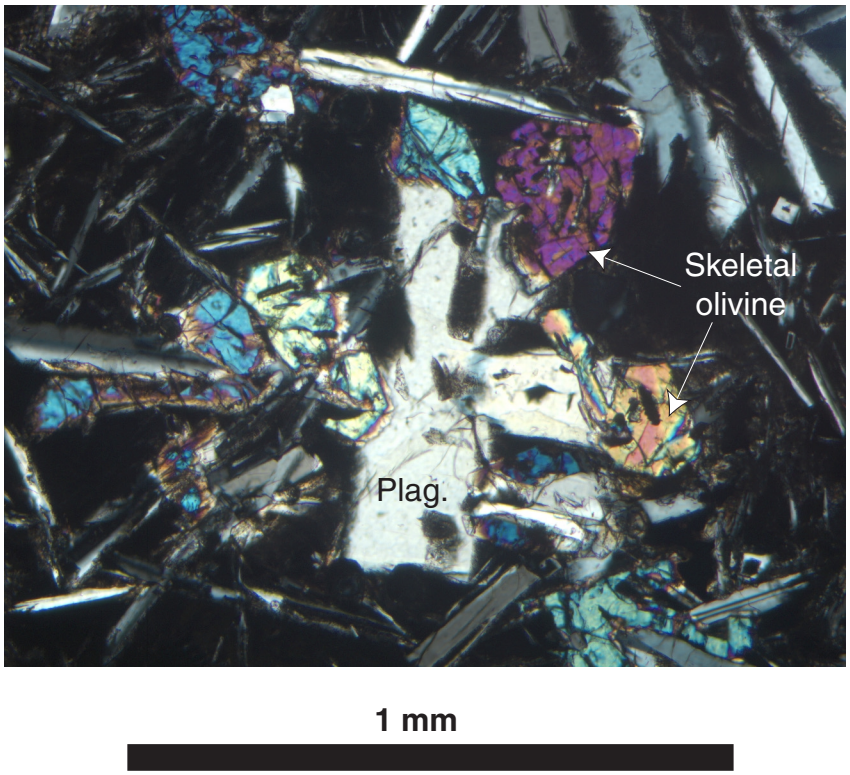

Figure F12. Photomicrograph of Sample 187-1164B-5R-1, 100–104 cm (see "Site 1164 Thin Sections," p. 25), showing tightly clustered tabular plagioclase forming a glomerocryst.

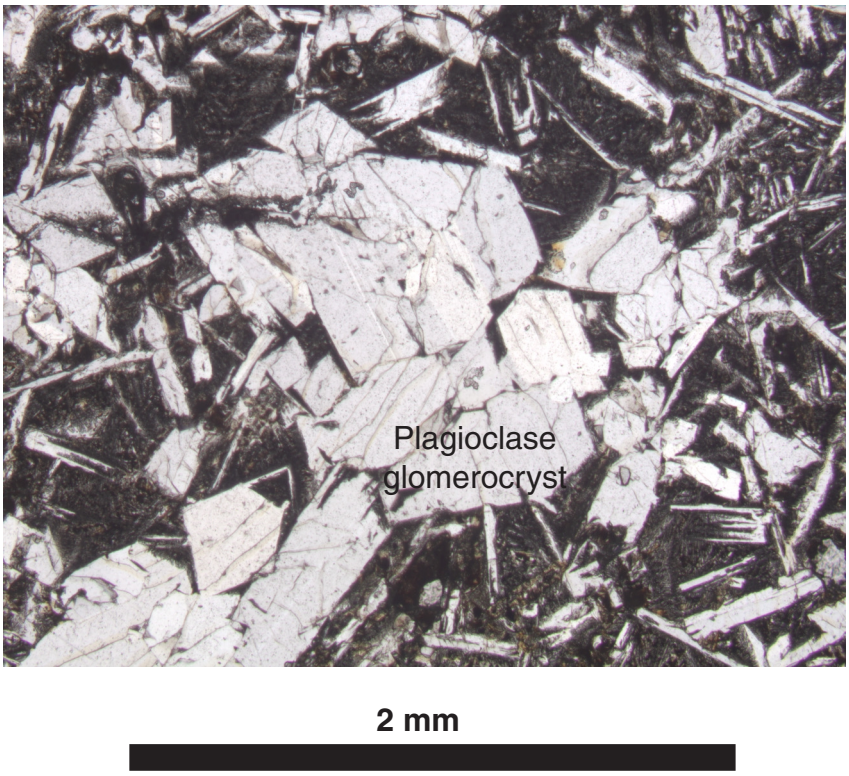

Figure F13. Photomicrograph in plane-polarized light of Sample 187-1164B-5R-1, 100–104 cm (see **"Site 1164 Thin Sections,"** p. 25), showing bladed habit of interstitial clinopyroxene in groundmass adjacent to a miarolitic cavity. Note the enhanced crystal growth of clinopyroxene in the miarolitic cavity relative to the rest of the groundmass.

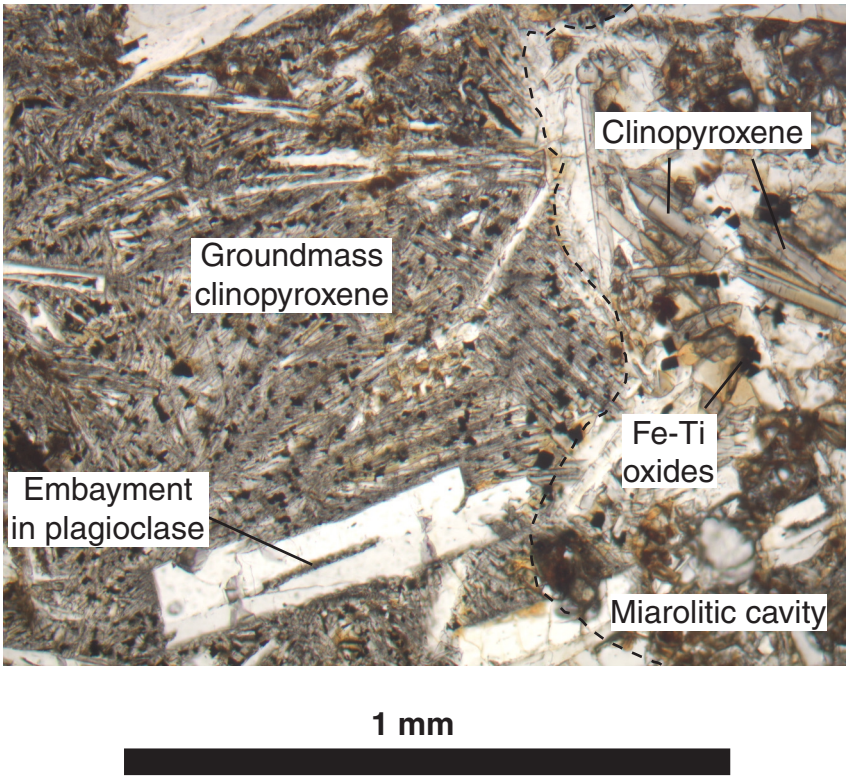

Figure F14. Photomicrograph in plane-polarized light of Sample 187-1164B-5R-1, 100–104 cm (see **"Site 1164 Thin Sections,"** p. 25), showing a miarolitic cavity with a multistage filling history. First, clinopyroxene crystals formed; then the remaining cavity was lined with Mn oxide before it was filled with calcite and Mn oxide.

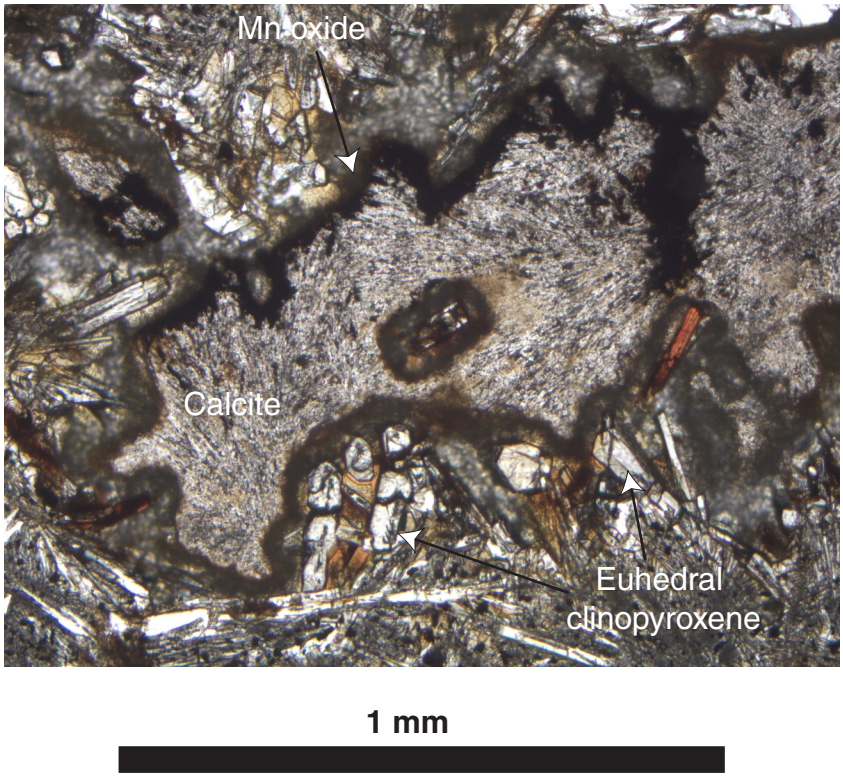

Figure F15. Photograph of interval 187-1164B-8R-1, 23–27 cm, showing an arcuate chilled margin on an aphyric pillow basalt clast with a classic V shape and short radial fractures through the glassy rind.

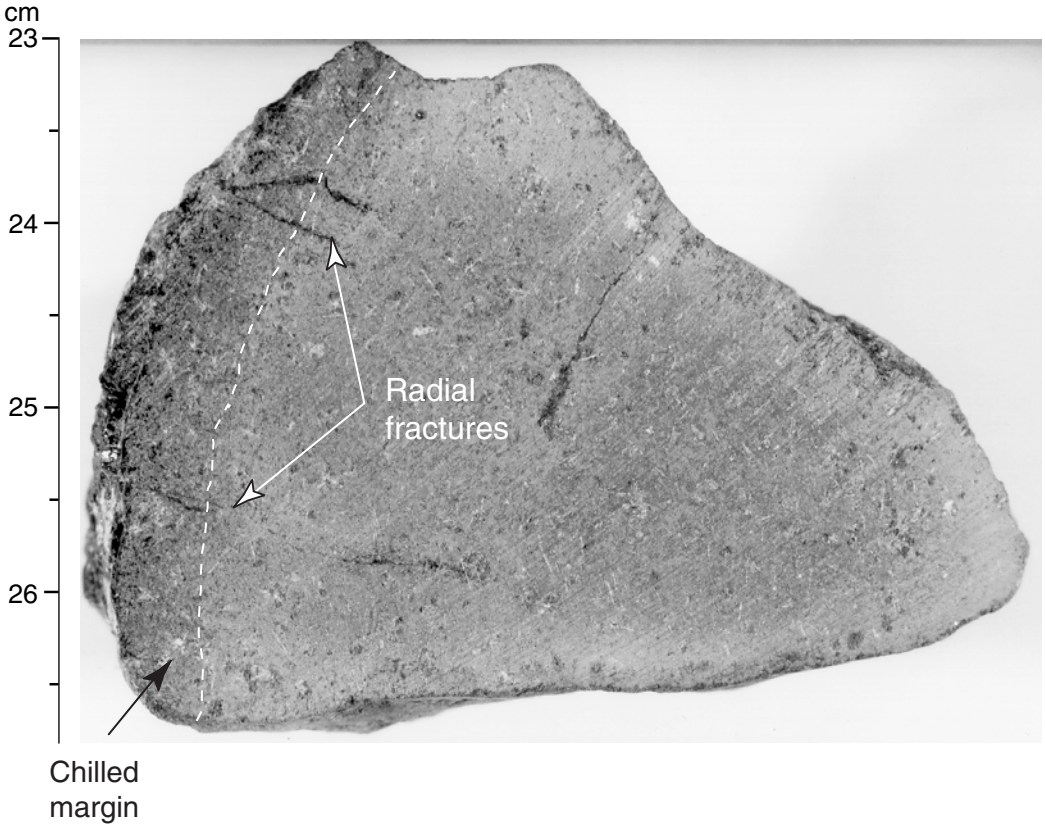

Figure F16. Photograph of interval 187-1164B-3R-1, 46–58 cm, showing palagonite-rich basaltic breccia adhering to aphyric basalt.

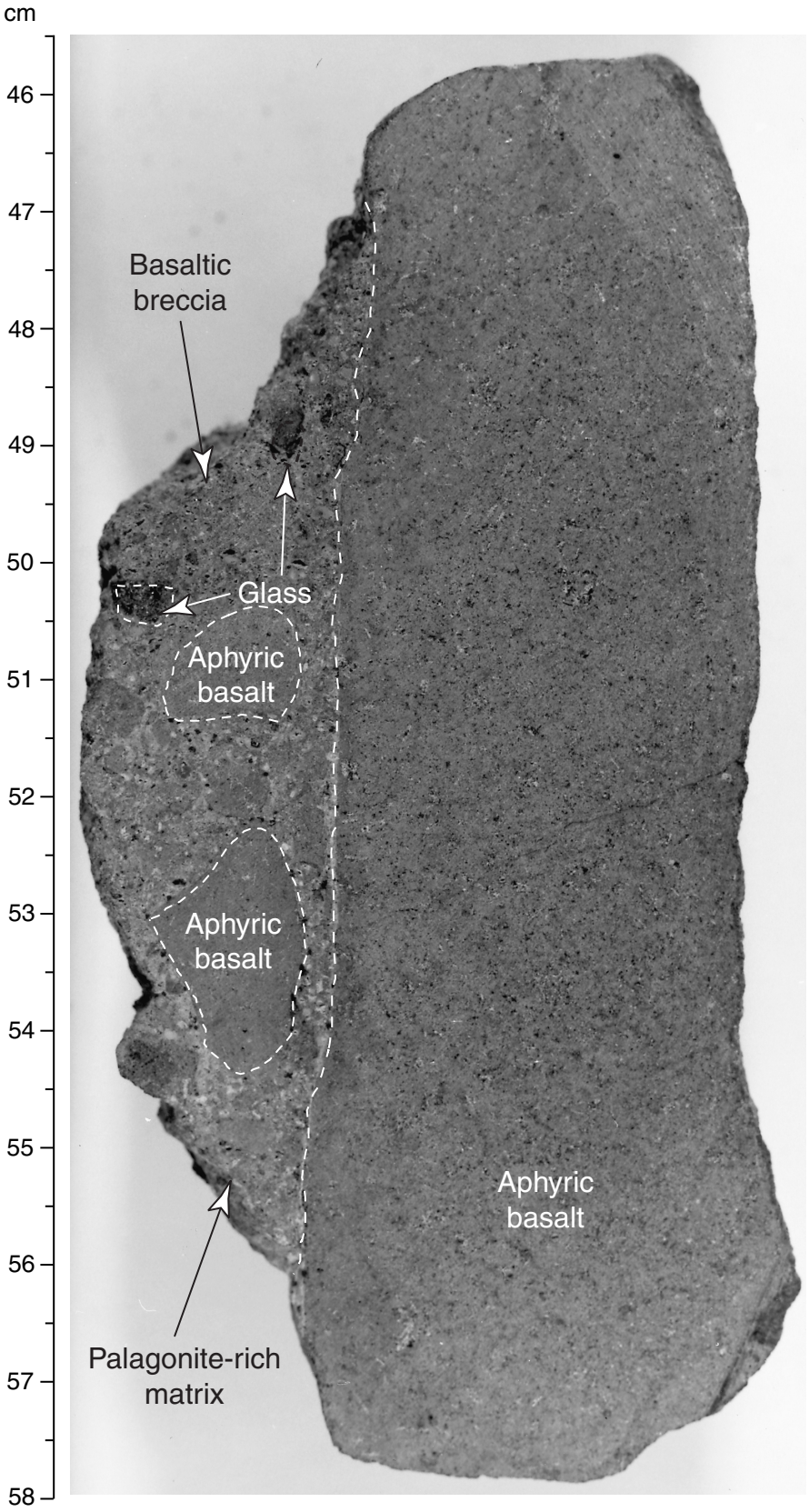

Figure F17. Photograph of interval 187-1164B-4R-2, 80–87 cm, showing palagonite-poor basaltic breccia clast.

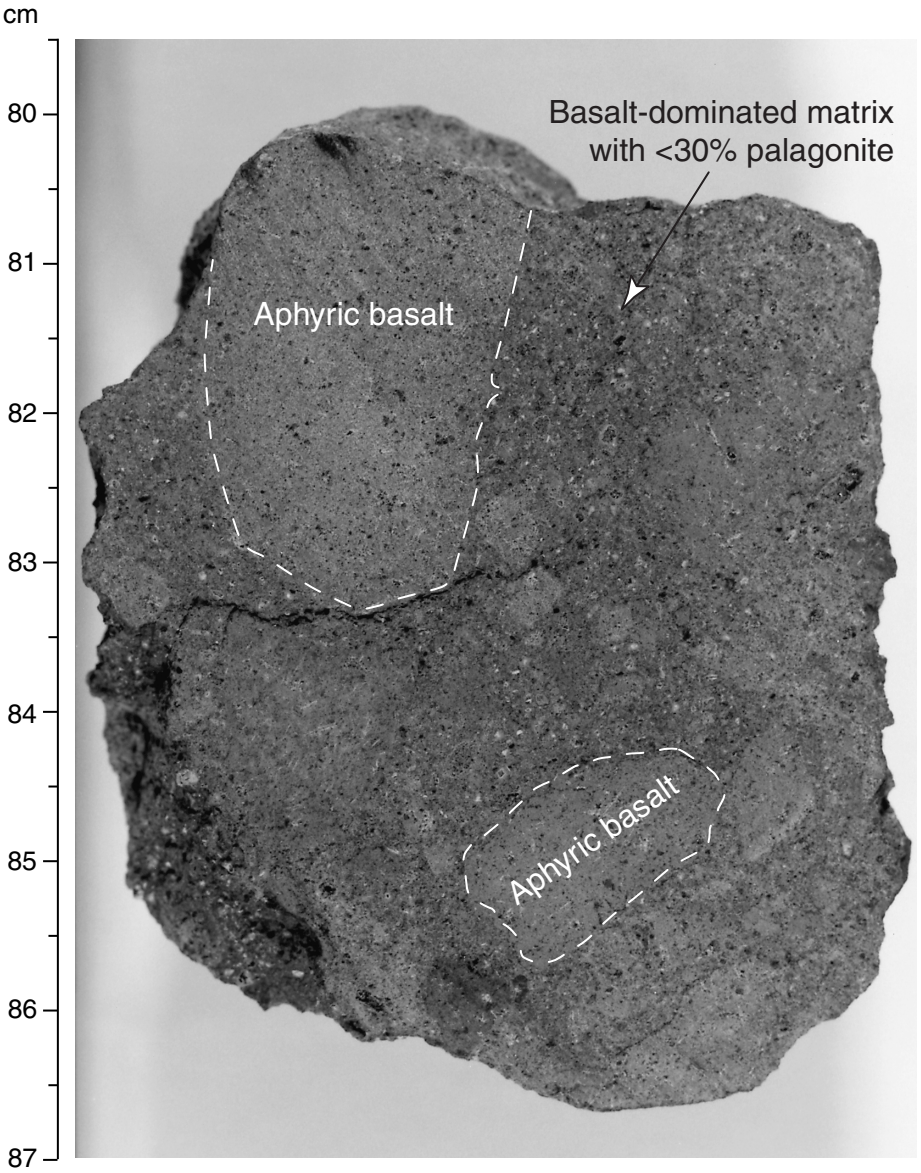

Figure F18. A. Photograph of interval 187-1164B-4R-2, 62–72 cm, the outside of the core piece, an aphyric basalt from Unit 1 of Hole 1164B with a chilled margin on the bottom and a layer of basaltic breccia on the top. Note the occurrence of finer grained sediment at the bottom of a pocket (center right) with coarser silt and sand-sized material overlying it. **B.** Photograph of interval 187-1164B-4R-2, 58–74 cm, which shows the cut face of the interval in Figure F18A. Figure F18A's pocket is shown as the small pocket (left) in this view.

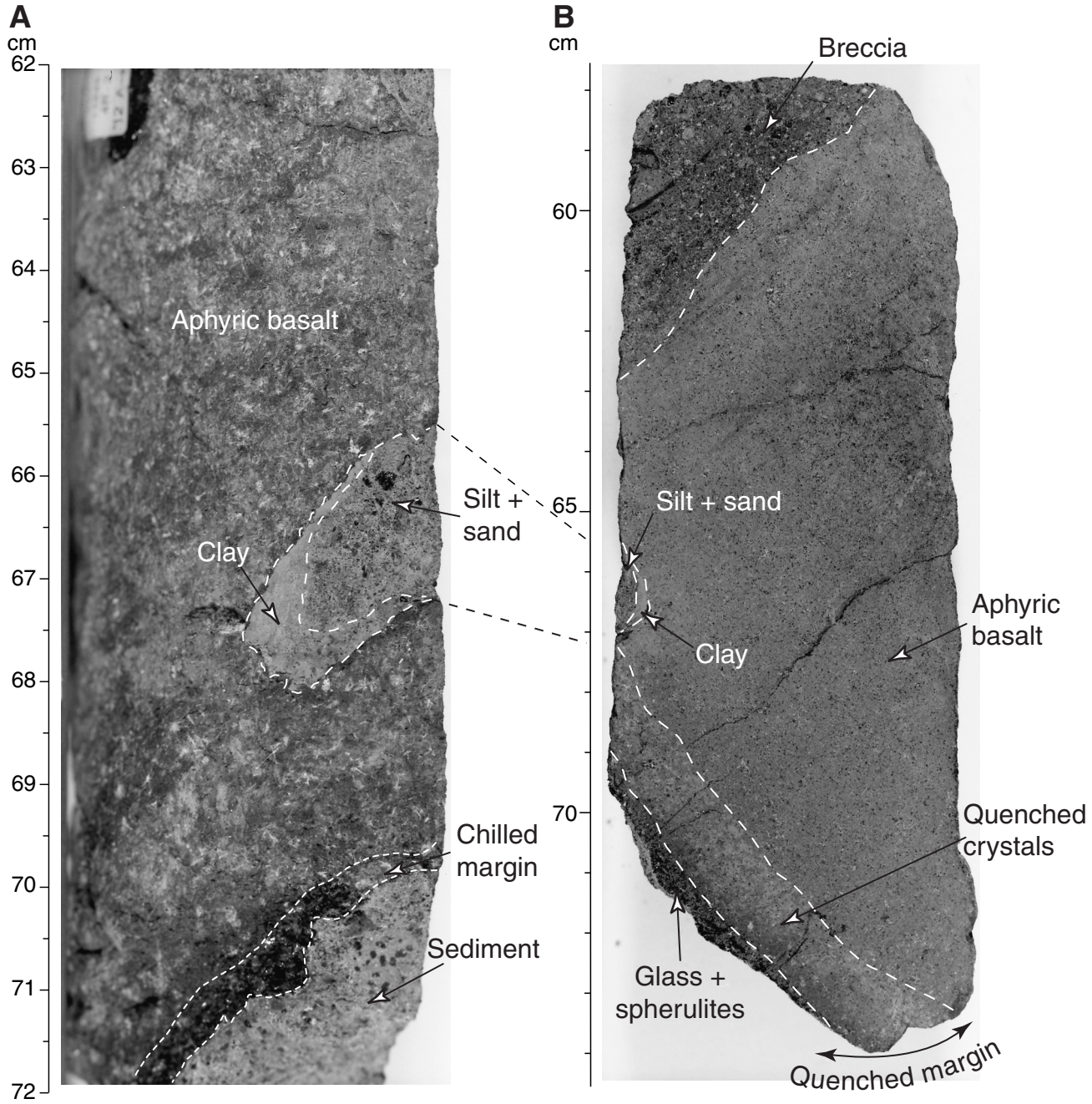

Figure F19. Photomicrograph in plane-polarized light of Sample 187-1164B-4R-2, 75–79 cm (see "Site 1164 Thin Sections," p. 24), showing palagonite-poor basaltic breccia with an abundance of unaltered, highly angular fragments of glass and olivine, as well as glass with palagonite rims and aphyric basalt. ol = olivine; gl = glass.

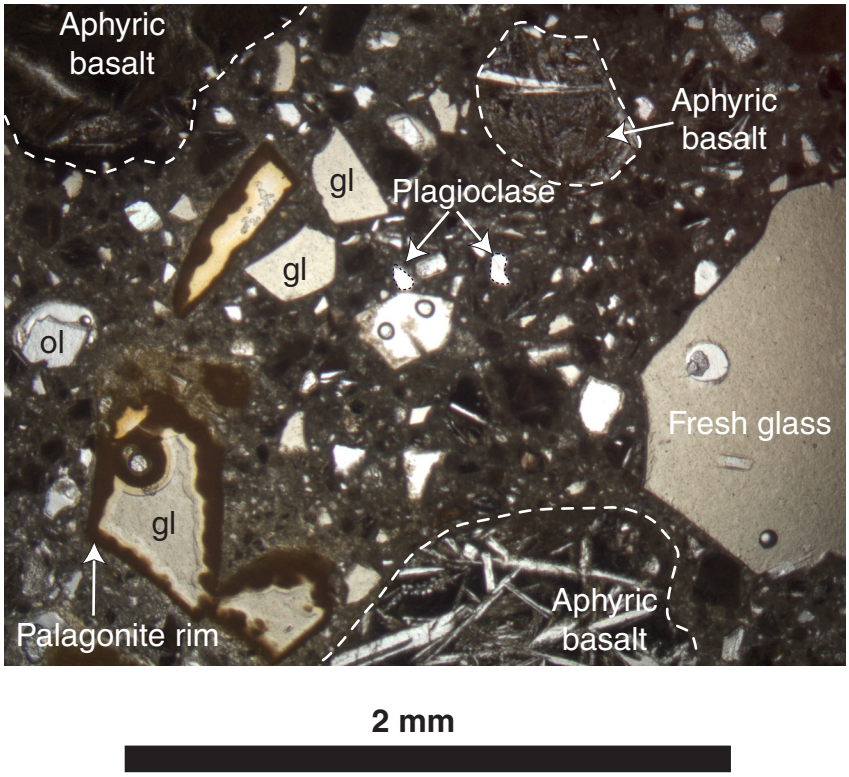

Figure F20. Photomicrograph, with crossed polars, of Sample 187-1164B-4R-2, 75–79 cm (see "Site 1164 Thin Sections," p. 24), showing basaltic breccia with an unresolvable clay + silt matrix and abundance of unaltered olivine crystals.

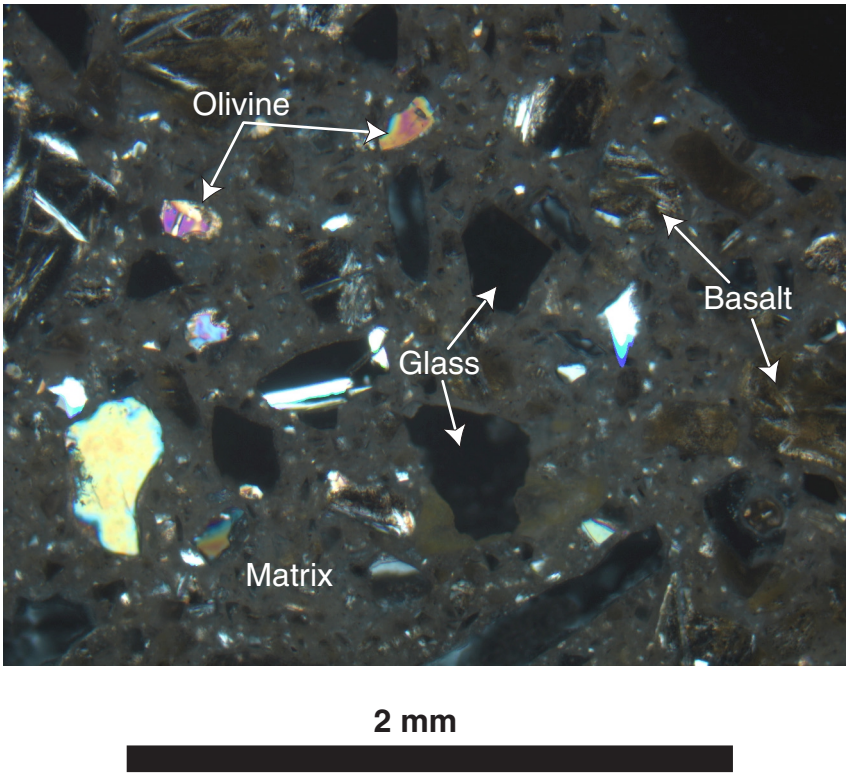

Figure F21. Photomicrograph, with crossed polars, of Sample 187-1164A-4R-1, 22–24 cm (see "Site 1164 Thin Sections," p. 21), showing patchy calcite replacing groundmass or, possibly, filling a vug.

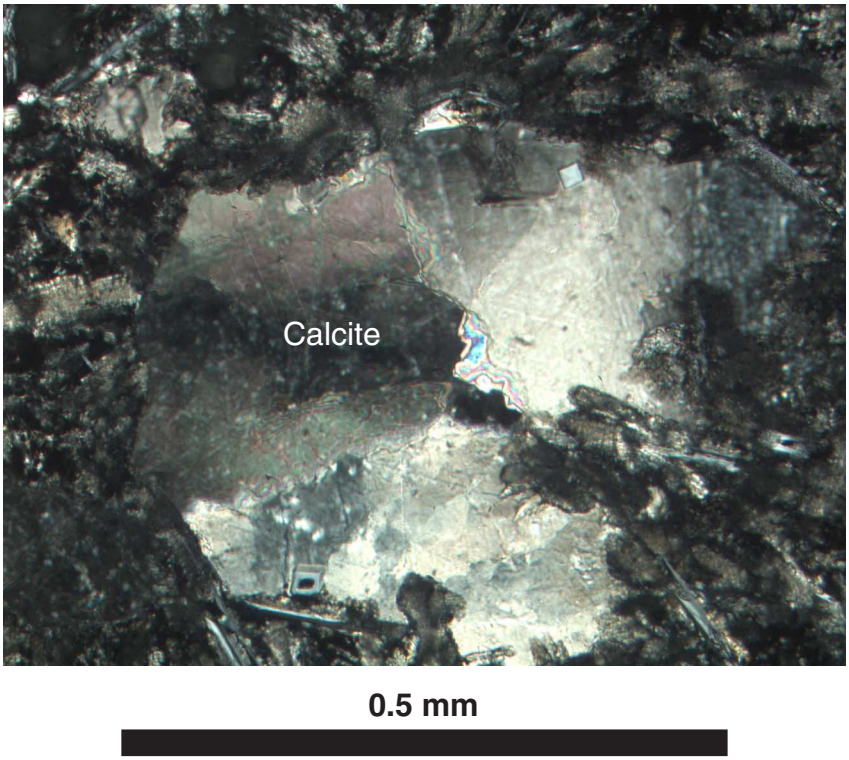

Figure F22. Photomicrograph, with crossed polars, of Sample 187-1164A-4R-1, 22–24 cm (see **"Site 1164 Thin Sections,"** p. 21), showing an olivine phenocryst partially replaced by calcite. Most calcite has been lost during sample preparation.

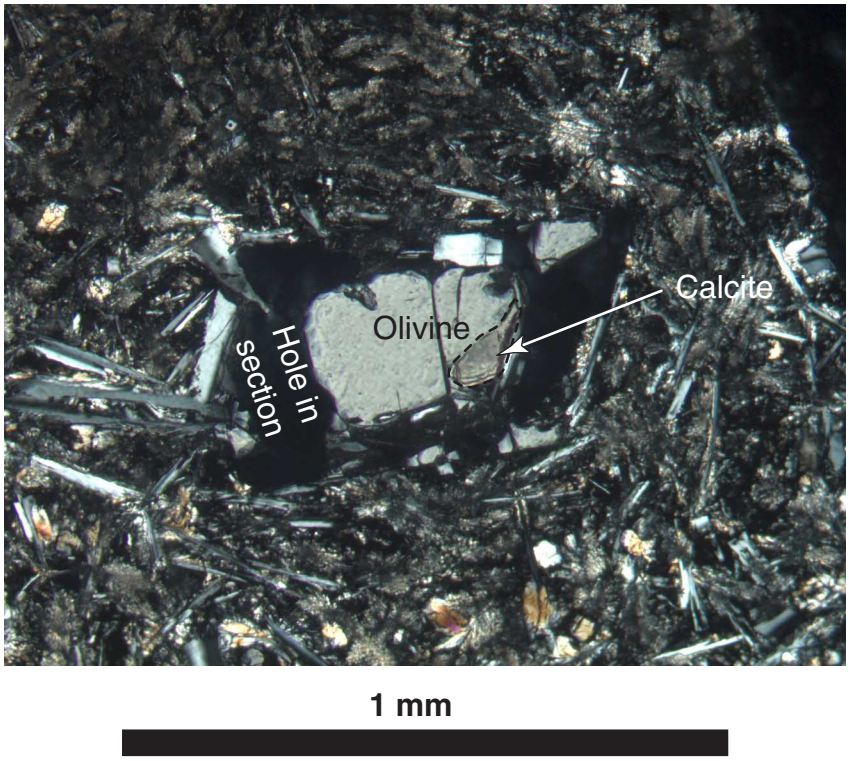

Figure F23. Photograph of interval 187-1164B-3R-2, 7–13 cm, showing a highly altered, sparsely plagioclase-olivine phyric basalt. Note the abundant groundmass olivine that is totally replaced by Fe oxyhydroxide and clay.

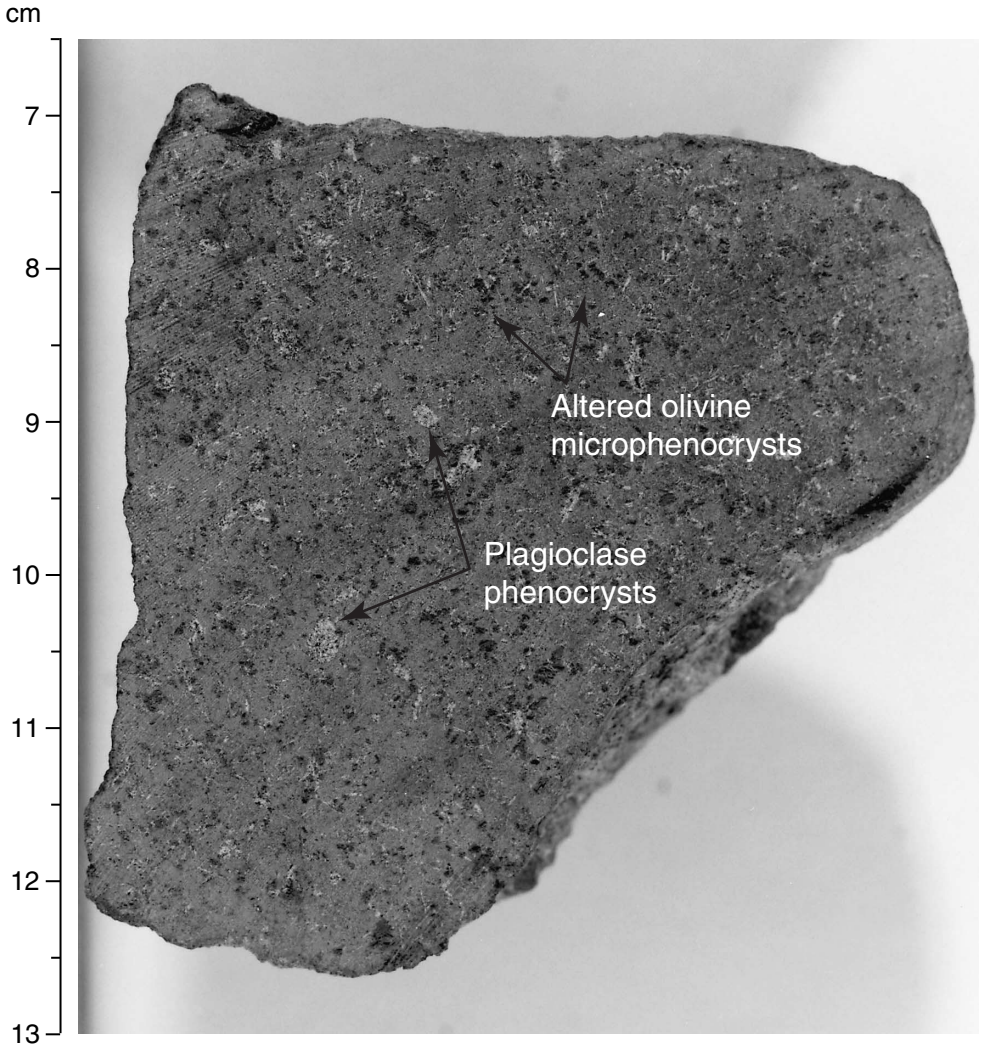

Figure F24. Photomicrograph in plane-polarized light of Sample 187-1164B-4R-1, 143–145 cm (see "Site 1164 Thin Sections," p. 23), showing pervasively altered groundmass of an aphyric basalt in which clinopyroxene and mesostasis are replaced by Fe oxyhydroxides and clay.

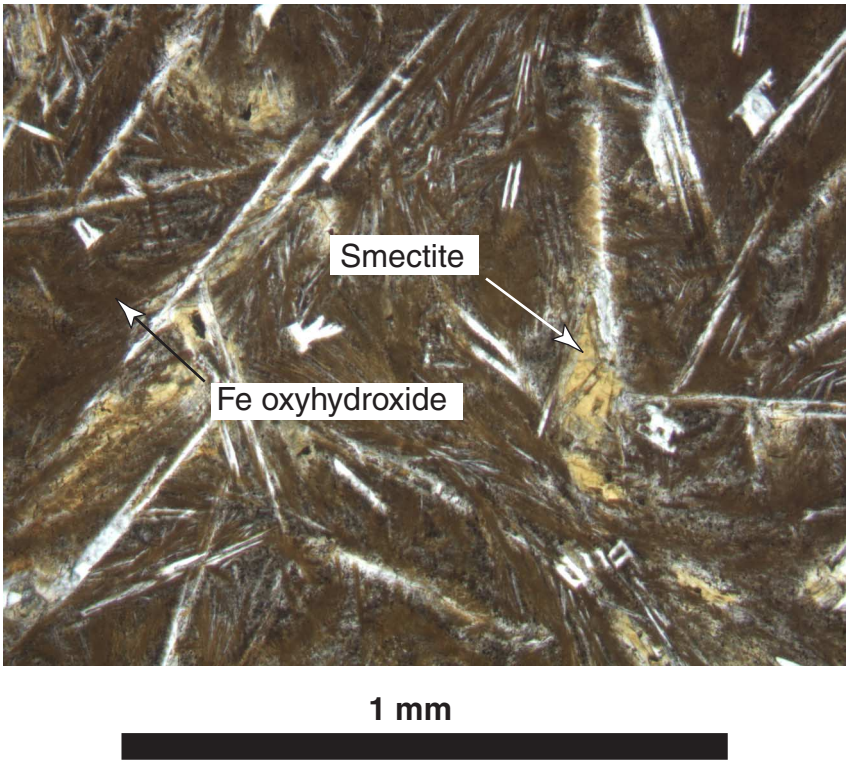

Figure F25. Photograph of interval 187-1164B-3R-2, 22–33 cm, showing a quenched pillow margin with 4 mm of fresh glass covered by a thin layer of orange-brown palagonite. The groundmass of the pillow interior is highly altered to Fe oxyhydroxide and clay. The dark patches are Mn oxide replacing groundmass.

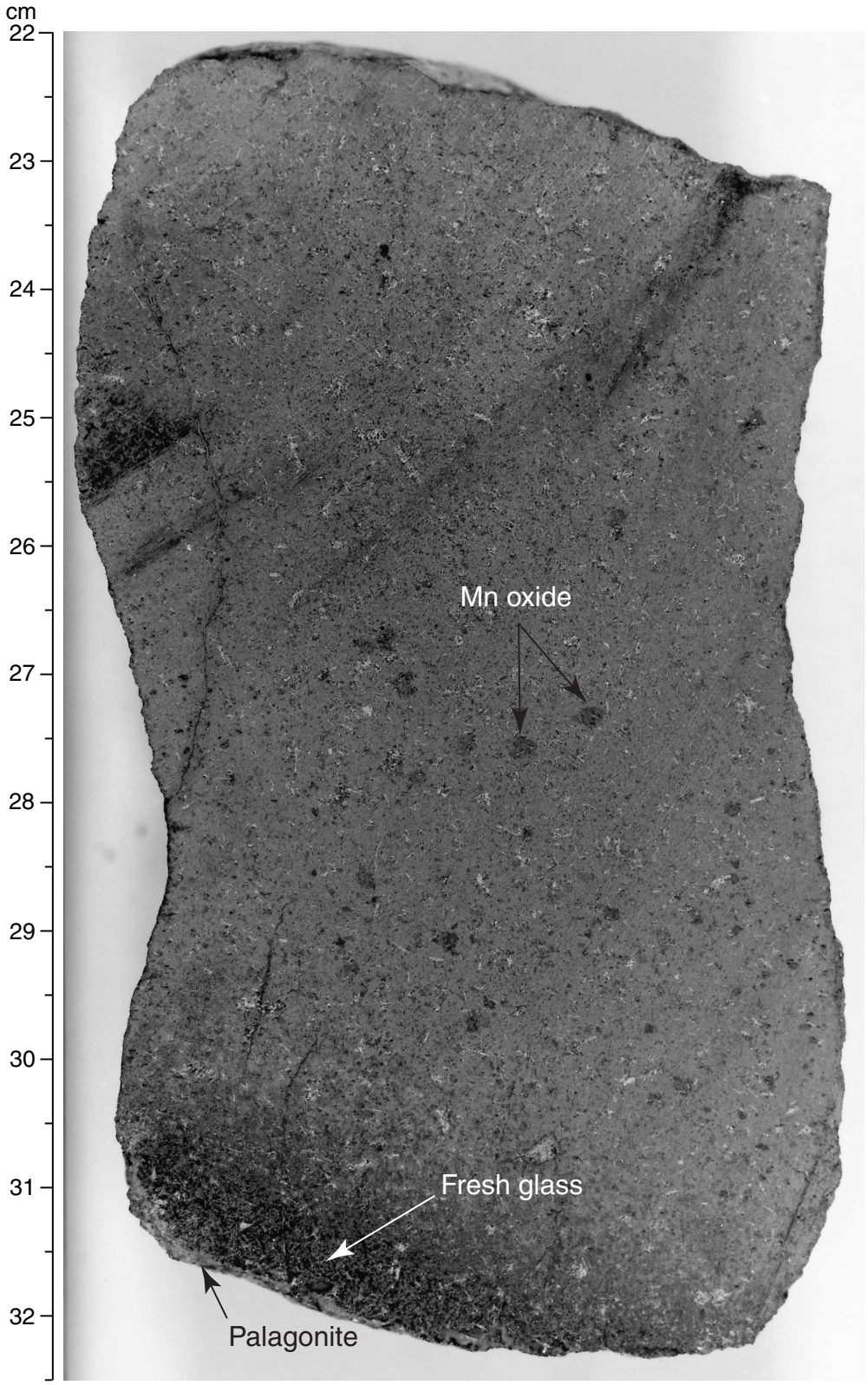

Figure F26. Photomicrograph in plane-polarized light of Sample 187-1164B-4R-2, 75–79 cm (see "Site 1164 Thin Sections," p. 24), showing fresh basalt shards without palagonite rims in the same basalt breccia as Figure F27, p. 39. The presence of both altered and fresh glass suggests that palagonitization predated brecia formation.

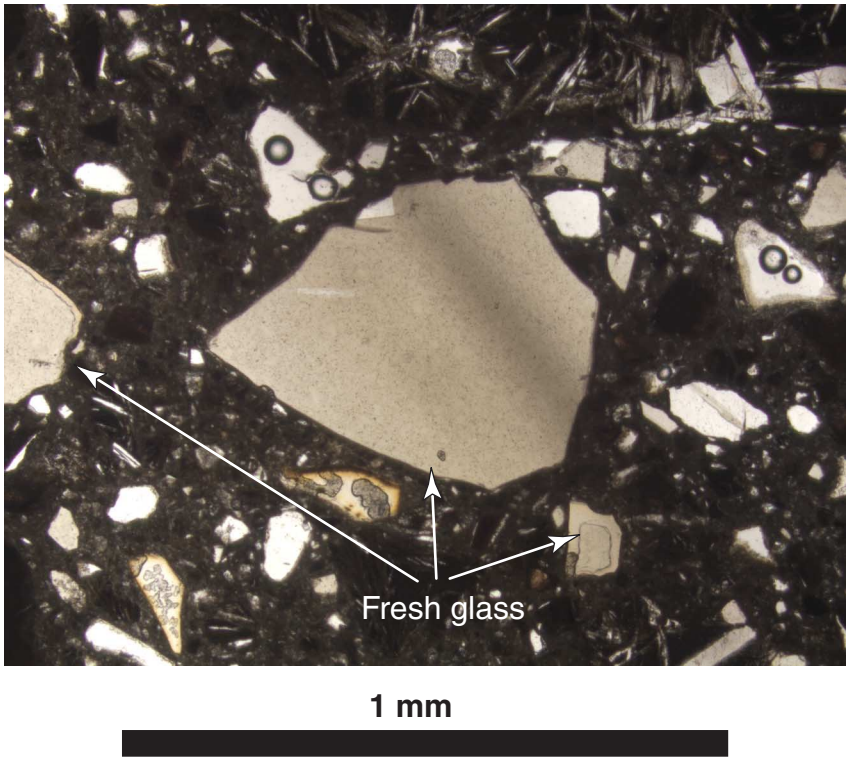

Figure F27. Photomicrograph in plane-polarized light of Sample 187-1164B-4R-2, 75–79 cm (see "Site 1164 Thin Sections," p. 24), showing a basalt glass shard with a fresh, clear core rimmed by dark brown palagonite in basalt breccia matrix. Note the absence of dendritic textures extending from the palagonite into the fresh glass.

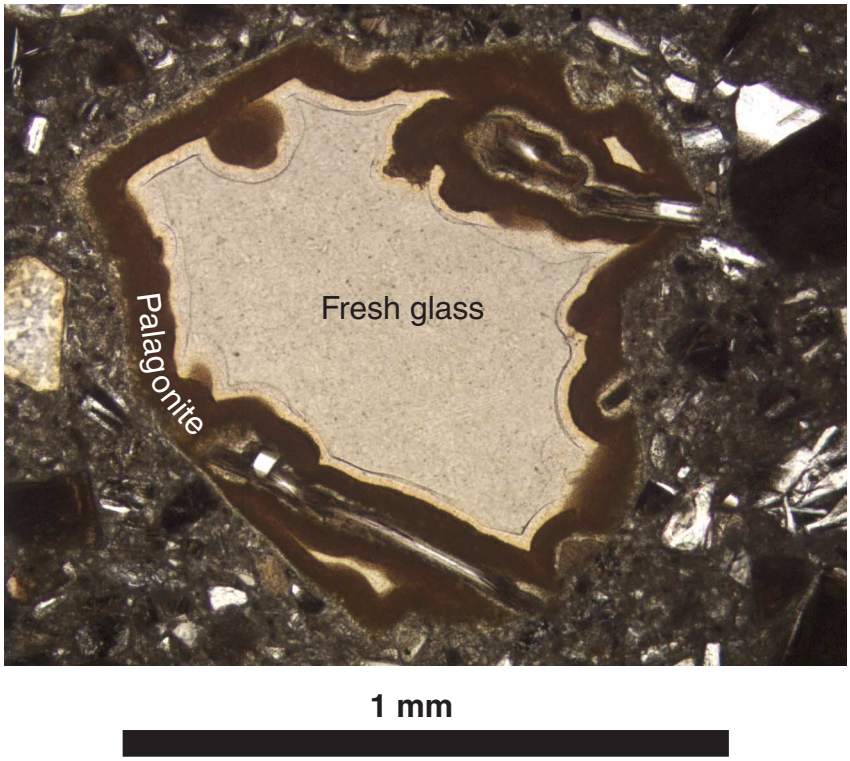

Figure F28. Track chart of the single-channel seismic survey line S12. Crosses = 50-shot intervals for line S12. Hole 1164A (solid circle) is located near shotpoint 136, almost identical with the proposed site, while Hole 1164B (solid circle) is 200 m southwest of shotpoint 136.

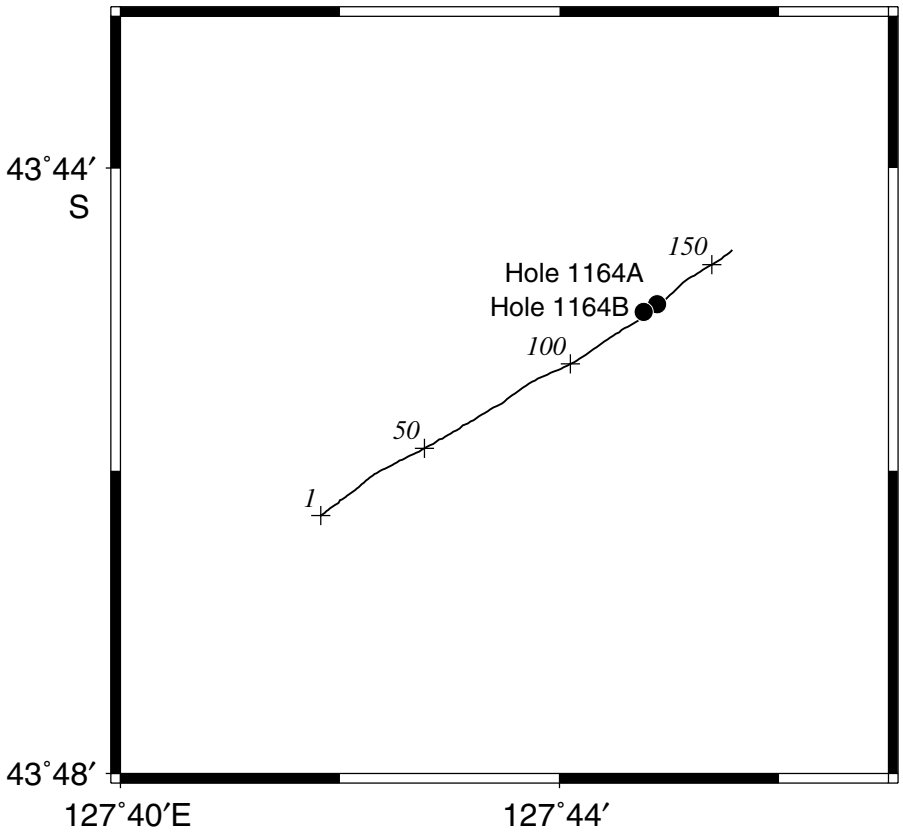

Figure F29. The single-channel seismic profile of line S12 from shotpoints 1 to 150. The heavy arrow marks the position of Site 1164 near shotpoint 136.

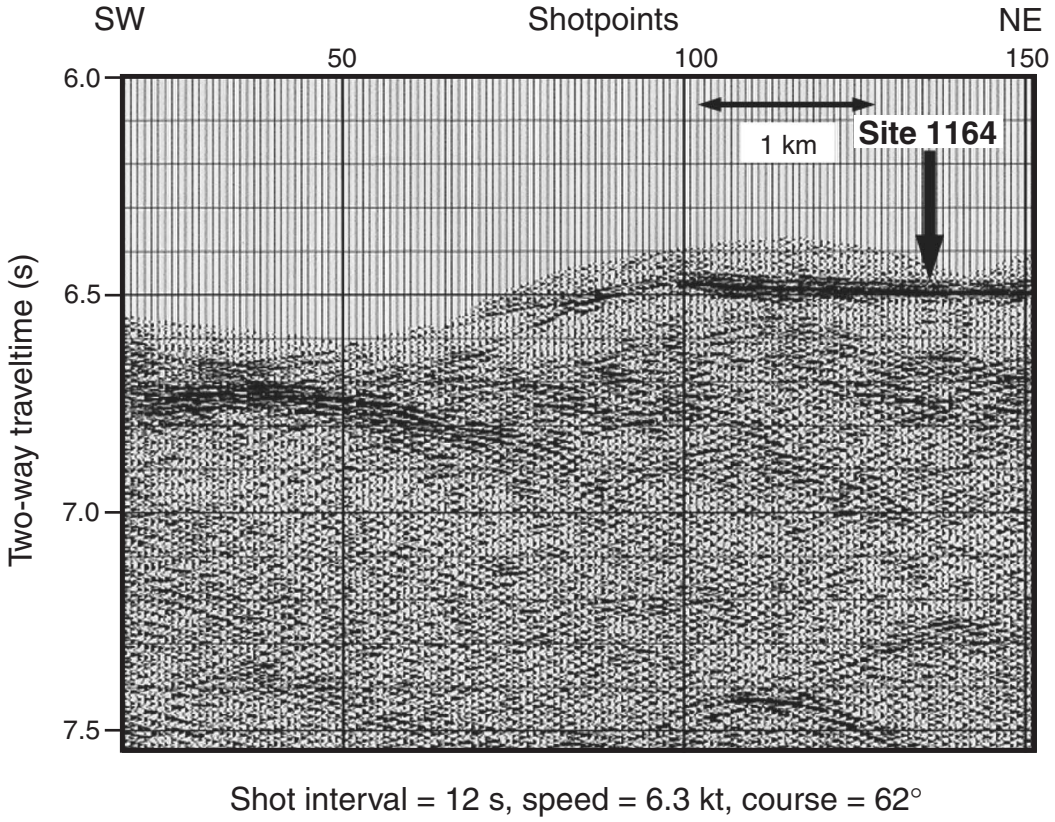

Figure F30. Major element variations vs. MgO for basalts from Holes 1164A and 1164B compared with Southeast Indian Ridge glasses from Segment B5. Only the average X-ray fluorescence or ICP-AES analyses reported in Table T4, p. 48, are plotted.

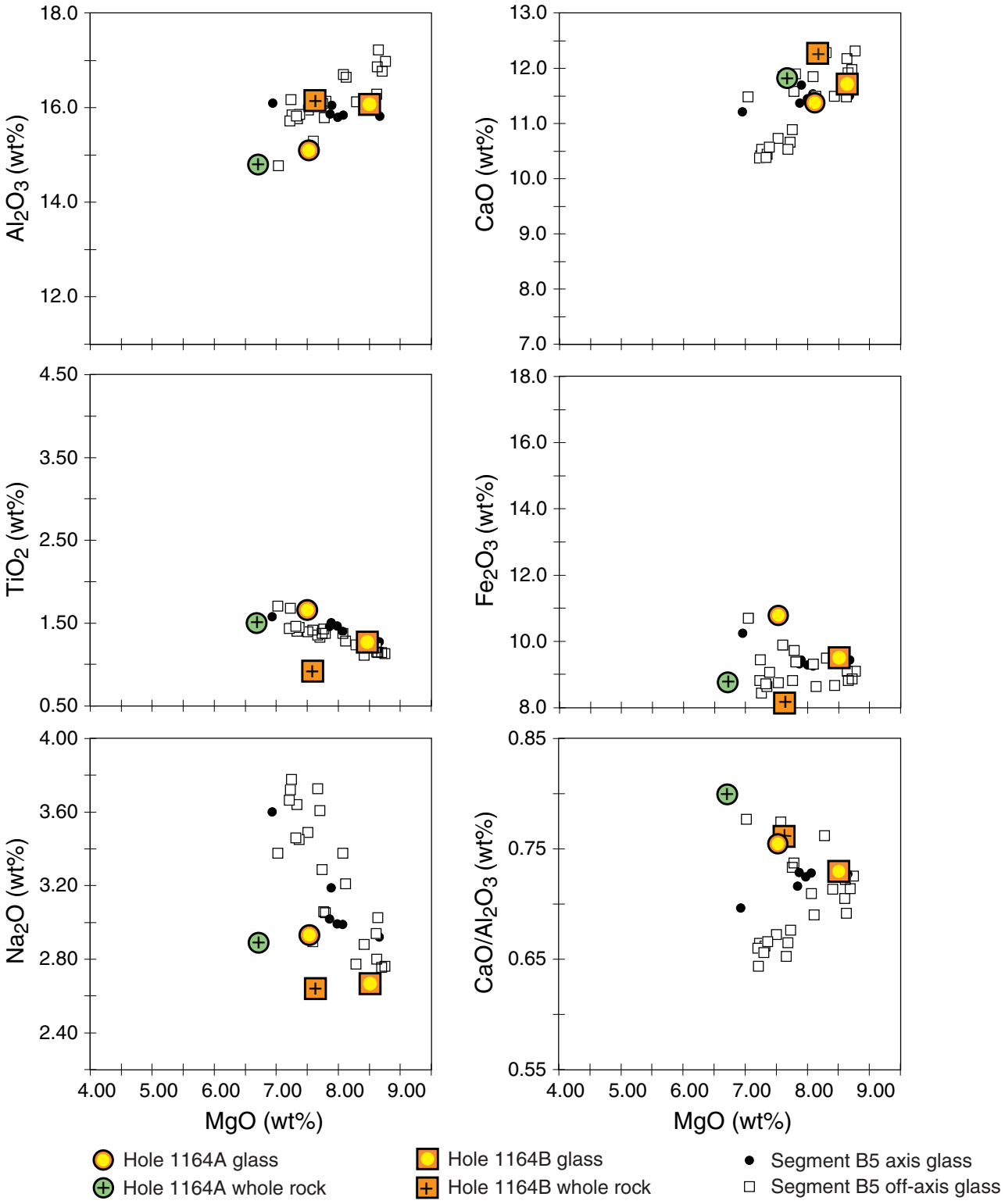

Figure F31. Trace element variations vs. MgO for basalts from Holes 1164A and 1164B compared with glasses from Segment B5.

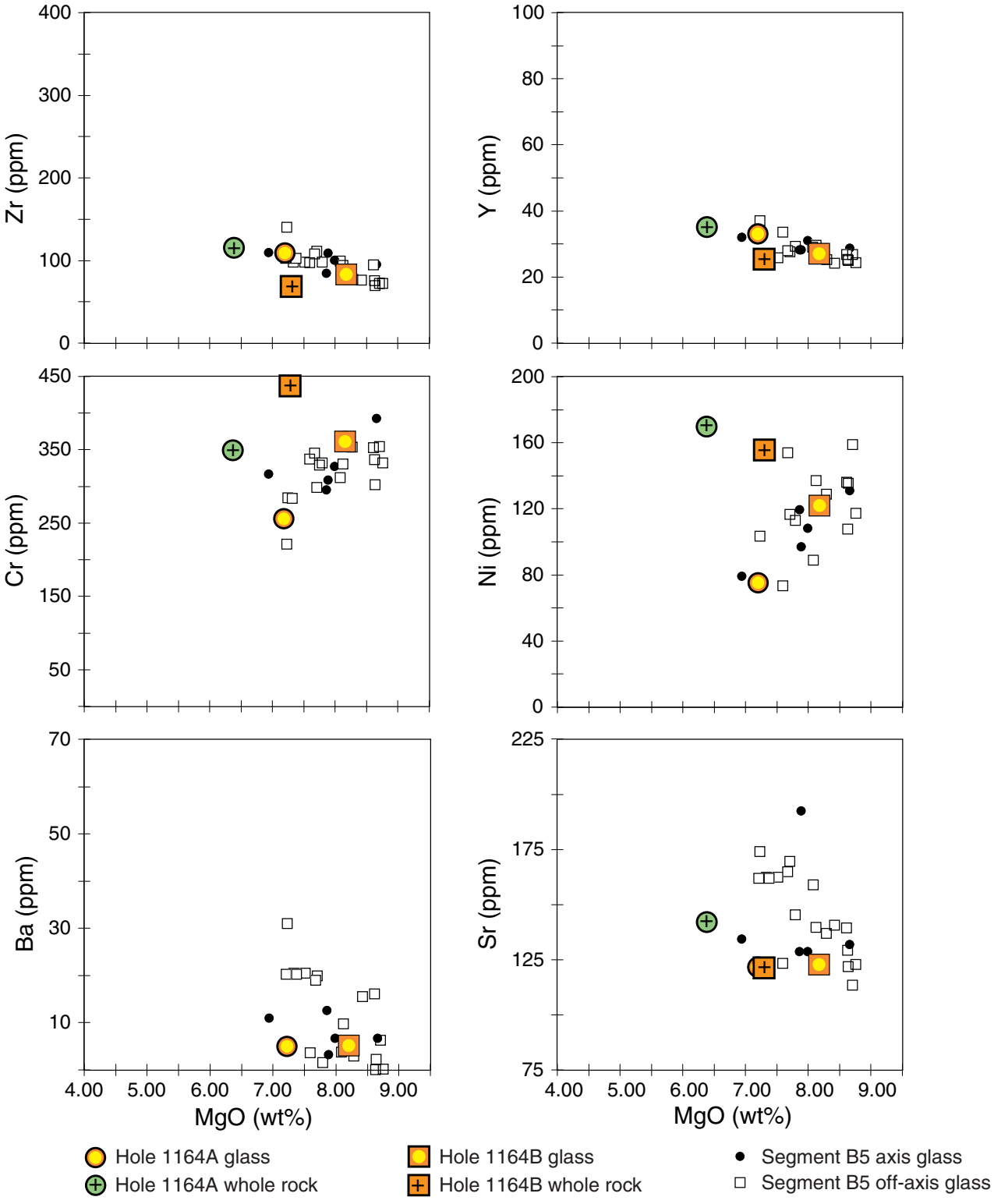

Figure F32. A. Variations of Zr/Ba vs. Ba ppm for Hole 1164A and Hole 1164B basaltic glass samples compared with Indian- and Pacific-type mid-ocean-ridge basalt (MORB) fields defined by zero-age Southeast Indian Ridge (SEIR) lavas dredged between 123°E and 133°E. TP = Transitional Pacific; PRT = propagating rift tip lavas. **B.** Variations of Na_2O/TiO_2 vs. MgO for Hole 1164A and Hole 1164B basaltic glass and whole-rock samples compared with Indian- and Pacific-type MORB fields defined by zero-age SEIR lavas dredged between 123°E and 133°E. Dashed line divides Indian- and Pacific-type domains based on zero-age SEIR basalt glass.

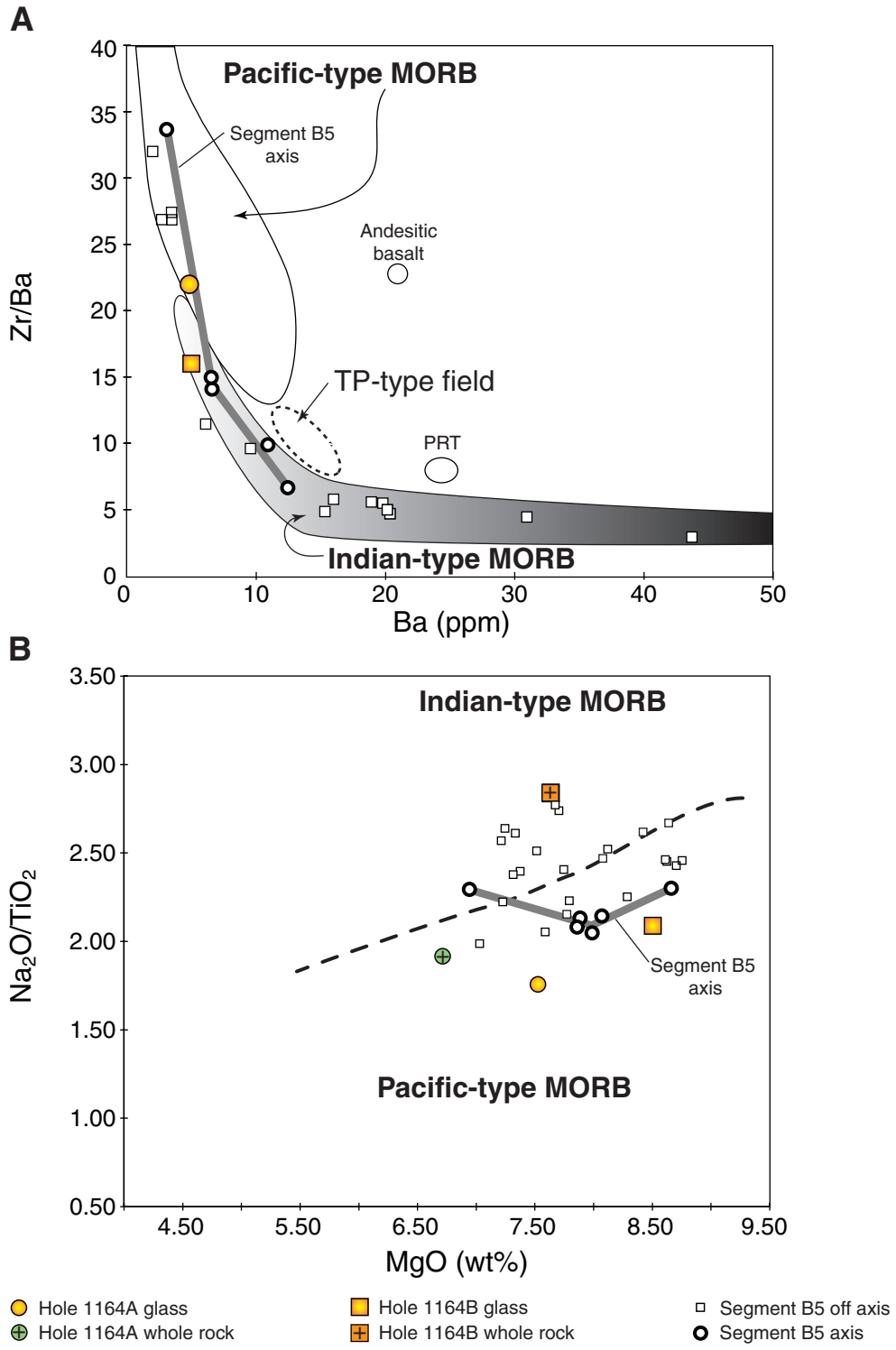

Table T1. Coring summary, Site 1164.

Hole 1164A
Latitude: 43°44.8998′S
Longitude: 127°44.8913′E
Time on hole: 1300 hr, 3 Jan 2000-1115 hr, 4 Jan 2000 (22.25 hr)
Time on site: 1300 hr, 3 Jan 2000-0900 hr, 6 Jan 2000 (6800 hr)
Seafloor (drill-pipe measurement from rig floor, mbrf): 4809.4
Distance between rig floor and sea level (m): 11.4
Water depth (drill-pipe measurement from sea level, m): 4798.0
Total depth (from rig floor, mbrf): 4956.4
Total penetration (mbsf): 147.0
Total length of cored section (m): 8.5
Total length of drilled intervals (m): 138.5
Total core recovered (m): 0.97
Core recovery (%): 11.4
Total number of cores: 3
Total number of drilled cores: 1

Hole 1164B
Latitude: 43°44.9521′S
Longitude: 127°44.7688′E
Time on hole: 1115 hr, 4 Jan 2000-0900 hr, 6 Jan 2000 (45.75 hr)
Seafloor (drill-pipe measurement from rig floor, mbrf): 4809.4
Distance between rig floor and sea level (m): 11.4
Water depth (drill-pipe measurement from sea level, m): 4798.0
Total depth (from rig floor, mbrf): 5025.5
Total penetration (mbsf): 216.1
Total length of cored section (m): 65.7
Total length of drilled intervals (m): 150.4
Total core recovered (m): 10.65
Core recovery (%): 16.2
Total number of cores: 9
Total number of drilled cores: 1

Core	Date (Jan 2000)	Ship local time	Depth (mbsf) Top	Depth (mbsf) Bottom	Length (m) Cored	Length (m) Recovered	Recovery (%)	Comment
187-1164A-								
1W	4	0255	0.0	138.5	138.5	0.75	N/A	
2R	4	0500	138.5	142.1	3.6	0.05	1.4	Whirl-Pak
3R	4	0830	142.1	146.7	4.6	0.63	13.7	
4R	4	1030	146.7	147.0	0.3	0.29	96.7	
				Cored:	8.5	0.97	11.4	
				Drilled:	138.5			
				Total:	147.0			
187-1164B-								
1W	4	1620	0.0	150.4	150.4	0.76	N/A	
2R	4	2030	150.4	155.8	5.4	0.47	8.7	Whirl-Pak
3R	4	2320	155.8	160.8	5.0	1.58	31.6	
4R	4	0230	160.8	170.2	9.4	2.03	21.6	
5R	4	0650	170.2	174.6	4.4	1.14	25.9	
6R	4	0930	174.6	179.3	4.7	0.87	18.5	
7R	4	1230	179.3	188.5	9.2	0.94	10.2	
8R	4	1500	188.5	197.5	9.0	1.16	12.9	
9R	4	1840	197.5	206.8	9.3	1.66	17.8	
10R	4	2250	206.8	216.1	9.3	0.80	8.6	Whirl-Pak
				Cored:	65.7	10.65	16.2	
				Drilled:	150.4			
				Total:	216.1			

Notes: N/A = not applicable. This table is also available in **ASCII** format.

Table T2. Relative abundance of moderately and highly altered basalt pieces, Hole 1164B.

Core	Total number of pieces	Highly altered		Moderately altered		Total (%)
		Number	(%)	Number	(%)	
187-1164B-						
1W-1	3	0	0	0	0	0
1W-2	5	1	20	1	20	40
2R-1	8	2	25	4	50	75
3R-1	20	3	15	8	40	55
3R-2	12	10	83		0	83
4R-1	25	21	84	4	16	100
4R-2	26	15	58	4	15	73
5R-1	31	27	87	4	13	100
6R-1	23	18	78	5	22	100
7R-1	24	10	42	14	58	100
8R-1	30	24	80	4	13	93
9R-1	25	5	20	20	80	100
9R-2	16	9	56	7	44	100
10R-1	14	2	14	1	7	21
Total:	262	147	56	76	29	85

Note: This table is also available in **ASCII** format.

Table T3. Rock samples incubated for enrichment cultures and prepared for DNA analysis and electron microscope studies and microspheres evaluated for contamination studies.

Core	Depth (mbsf)	Sample type	Enrichment cultures			DNA analysis			SEM/TEM samples		Microspheres*	
			Anaerobic	Aerobic	High pressure	Wash	Centrifuged	Fixed	Fixed	Air dried	Exterior	Interior
187-1164A-												
2R	138.5-142.1										Yes	X†
187-1164B-												
2R	150.4-155.8										Yes	Yes
3R	155.8-160.8	Breccia with chilled margin	9	3	X	X		X	X	X		
8R	188.5-197.5	Chilled margin	8	3		X		X		X		
10R	206.8-216.1	Chilled margin	7	1	X	X		X	X	X	Yes	Yes
		Seawater					X	X				

Notes: SEM = scanning electron microscope; TEM = transmission electron microscopy; * = contamination test; X = samples prepared on board; † = no thin sections were made to examine the interiors of the rocks for microspheres. This table is also available in **ASCII** format.

Table T4. Glass and whole-rock major and trace element compositions of basalts, Site 1164.

	Hole 1164A				Hole 1164B			
Core, section:	2R-1	2R-1	4R-1	4R-1	1W-1	1W-1	2R-1	2R-1
Interval (cm):	1-5	1-5	20-24	20-24	41-43	41-43	53-56	53-56
Depth (mbsf):	138.51	138.51	146.9	146.9	0.41	0.41	150.93	150.93
Piece:	1	1	4	4	1	1	7	7
Analysis:	ICP	ICP	XRF	XRF	ICP	ICP	XRF	XRF
Rock type:	Glass	Glass	Aphyric basalt		Glass	Glass	Sparsely to moderately plagioclase-olivine phyric basalt	
Major element (wt%)								
SiO_2	53.04	51.58	50.64	51.02	52.32	50.92	48.97	48.80
TiO_2	1.68	1.66	1.53	1.49	1.30	1.26	0.90	0.96
Al_2O_3	15.02	15.16	14.77	14.81	16.00	16.12	16.12	16.15
Fe_2O_3	11.06	10.55	8.74	8.78	9.58	9.44	8.14	8.14
MnO	0.16	0.17	0.16	0.15	0.15	0.16	0.11	0.12
MgO	7.57	7.49	6.67	6.75	8.53	8.49	7.65	7.62
CaO	11.28	11.52	11.76	11.90	11.65	11.79	12.31	12.27
Na_2O	2.94	2.92	2.83	2.95	2.63	2.71	2.66	2.62
K_2O	0.11	0.12	0.26	0.26	0.09	0.09	0.20	0.19
P_2O_5	0.16	0.17	0.15	0.15	0.14	0.13	0.09	0.09
LOI			0.53	0.53			1.09	1.09
CO_2								
H_2O	103.01	101.32	98.04	98.79	102.38	101.10	98.24	98.05
Total:								
Trace element (ppm)								
Nb			5				4	
Zr	105	113	115		80	85	68	
Y	30	36	35		25	29	25	
Sr	117	127	142		116	129	121	
Rb			2				4	
Zn			81				66	
Cu			99				69	
Ni	73	77	170		122	121	156	
Cr	244	268	349		355	367	437	
V			265				201	
Ce			30				15	
Ba	4	6			5	6		
Sc	38	39			32	36		

Notes: LOI = loss on ignition. This table is also available in **ASCII** format.